Implementation of faster than Nyquist signaling on LTE-uplink like system models

By

Antriksh Awasthi

Department of Electrical and Information Technology
Faculty of Engineering, LTH, Lund University
SE-221 00 Lund, Sweden
&
Huawei Technologies Sweden, AB
SE-164 40 Kista,Stockholm

Advisors: Fredrik Rusek & Tommy Zhongmin Deng

Acknowledgements

First and foremost, I would like to express my gratitude towards my supervisor, Fredrik Rusek, for providing me with an opportunity to work on this thesis. I would have never imagined finishing this thesis without his able guidance and support. I appreciate his candour and straightforwardness and hope that everything I have learnt from him as a student and at a personal level will always stay with me and guide me in my later years.

Secondly, I would like to thank my mentor and manager at Huawei Technologies Sweden, AB, Tommy Zhongmin Deng, for providing me with an opportunity to work on this project with the company. Tommy has been very supportive and his encouragement and motivation helped me keep going. While working in Huawei, I had a chance to interact with diverse people who guided me with my project as well as career front. Also, I would like to specially thank Dr. Shousheng He for all the technical talks and suggestions.

I would like to thank my family and friends without them I won't even exist. The financial and emotional support provided by my family made it possible for me to come all the way from a small town in India to study in Sweden. It is indeed, once in a lifetime experience.

Last but not the least, I would to thank my girlfriend, Ruby, for always staying by my side and reminding me of all the positive things in this world.

Antriksh Awasthi

Abstract

As the data rate requirements are increasing rapidly, so is the need to design better bandwidth efficient digital communication systems. Higher bandwidth efficiency can be achieved by different methods, but in this thesis we procured it by increasing the data rates beyond the Nyquist rate while keeping the bandwidth constant. This approach of increasing the data rate beyond the Nyquist rate is called faster than Nyquist signaling or simply FTN. In FTN the transmitted data symbols in time domain are disturbed by the controlled amount of interference from the neighboring symbols known as the intersymbol interference (ISI). This technique of intentionally sending the data sequence affected by the controlled amount of ISI was first put forth by James Mazo in 1975. Since then the research in the field of FTN has been extended in many directions.

The LTE-uplink system is based on single carrier transmission and can be extended to the faster than Nyquist signaling to achieve better bandwidth efficiency. The aim of this thesis is to implement the FTN on an LTE-uplink like system model and compare it with the traditional LTE-uplink system. The performance of the systems is compared on the basis of bit error rates (BER) and spectral efficiency. The mathematical model for the FTN signaling have been derived according to the 'Ungerboeck model' and 'Forney model' for the Nyquist based systems. Moreover two separate cases are presented, the uncoded FTN and coded FTN. In the uncoded case, for the optimal detection (ML detection) of the received FTN signal sequence we used a sphere decoder. In the coded case, we have used a LDPC encoder of code rate $\mathrm{R_c} = \frac{1}{2}$ at the transmitter side and a soft-input-soft-output MMSE equalizer cascaded with an iterative LDPC decoder at the receiver side.

Table of Contents

List of Figures

Chapter 1

Introduction

1.1 Background

Digital communication systems of the present day are all architecturally based on a landmark theory given by Claude Shannon [1] in 1948, famously known as Information theory. Information theory has been serving as the basis of architectural design in almost every digital communication system since the early 70's. Advancements in digital hardware according to *Moore's law* pushed the practical implementation of Information theory.

The idea of converting source information into digital bits, process them and convert them back to continuous signals just before transmission, without any loss of generality, was a revolutionary idea which stimulated the development in this field to a new height. For example, the shift from 1st generation (AMPS) to 2nd generation (GSM) mobile communication systems noticed a huge jump in spectral efficiency from .001 bit/sec/Hz/Cell to .17 bit/sec/Hz/Cell [29].

A strictly bandlimited nature of physical channels extends the signals in the time domain which leads to inter-symbol interference (ISI). For the ISI free reception of the signals the waveforms representing the symbols shall be orthogonal to each other at every time instance and the waveforms satisfying this property are known as ideal Nyquist pulses. Harry Nyquist, while working in Bell labs, published a benchmark paper *Certain Topics in Transmission Theory* [2]. Nyquist provided a criteria for the waveforms to be ideal Nyquist. This is also known as the Nyquist criterion. The Nyquist criterion served as the base of communication system design for a long time, which was based on the waveforms representing uncoded symbols. Later Shannon extended the Nyquist criteria for the coded data symbols as well.

Most of the communication systems of the present day are based on the

Nyquist criterion and trying to approach Shannon's capacity limit. There still persists a challenge to reliably communicate information via digital communication channel models with highest possible rate, i.e., to reach capacity. There is a possibility to increasing the spectral efficiency by discarding the Nyquist orthogonality criterion. That is by sending the transmit pulse at a rate faster than the Nyquist rate. The history of faster than Nyquist (FTN) signaling started when James Mazo published [3] in 1975. Mazo accelerated *sinc* pulses beyond the Nyquist rate and found some astonishing results.

1.2 Thesis goals

This *master's thesis* is an attempt to understand and exploit the underlying basic principles of digital communication and their applications in the area of FTN signaling. The main goals of this thesis are as following:

- Derive the discrete time mathematical model for the FTN signaling.
- Compare the Nyquist based LTE-uplink transmission scheme with the FTN based approach.
- Study the trade-offs for implementing FTN signaling on LTE-uplink system model.

1.3 Channel capacity & bandwidth efficiency for an AWGN channel and faster than Nyquist approach

Shannon gave the fundamental equation to calculate the maximum amount of information an AWGN channel can carry with arbitrarily low error probability. He named it channel capacity C, and is measured in bits/sec. Capacity is the ultimate limit, and he stated that it is possible to approach capacity with sophisticated coding schemes. However it is impossible to carry information at a rate above capacity with low error probability. Recently, channel coding schemes like LPDC and turbo codes have impressively approached capacity. If the bandwidth is limited to W in Hz, power is limited to P in Watts and the noise power spectral density is N_0 in Watts/Hz, then the channel capacity C for an additive white Gaussian noise channel is given by,

$$C = W \log_2 \left(1 + \frac{P}{N_0 W}\right). \tag{1.1}$$

The capacity C increases monotonically with W and reaches its highest value of $\frac{P}{N_0} \log_2 e$ as $W \to \infty$. Eq. (1.1) provides the upper bound for the

rate of reliable communication R, such that $R \leq C$. Therefore, data rate R is given by,

$$R \leq W \log_2 \left(1 + \frac{P}{N_0 W}\right). \tag{1.2}$$

If a long code is chosen randomly at a rate R then there exists a decoder such that communication can be carried out at a relatively small error probability approaching to zero. Another term, $\frac{E_b}{N_0}$ is more important and used quite often in practice to compare the performance of different communication systems, where, E_b is defined as the energy per information bit. The relation between $\frac{E_b}{N_0}$ and spectral efficiency η in bits/(s − Hz) is quite trivial and can be easily derived from eq. (1.2). By substituting $\eta = \frac{R}{W}$ and $P = E_b R$ in eq. (1.2), we get,

$$\begin{aligned}
\frac{R}{W} &\leq \log_2 \left(1 + \frac{E_b R}{N_0 W}\right), \\
\eta &\leq \log_2 \left(1 + \frac{\eta E_b}{N_0}\right), \\
\frac{E_b}{N_0} &\geq \frac{2^\eta - 1}{\eta}.
\end{aligned}$$

If $\left\{\frac{E_b}{N_0}\right\}_{min}$ is the minimum value of $\frac{E_b}{N_0}$, then we can write the above equality as,

$$\frac{E_b}{N_0} \geq \left\{\frac{E_b}{N_0}\right\}_{min} = \frac{2^\eta - 1}{\eta}, \tag{1.3}$$

where $\left\{\frac{E_b}{N_0}\right\}_{min}$ decreases monotonically with decreasing η and approaches $\log_e 2$ (-1.59 dB) as $\eta \to 0$, which is also known as the ultimate Shannon limit on $\frac{E_b}{N_0}$ for any η. However, there is a requirement on η to be as large as possible for a smallest possible value of $\left\{\frac{E_b}{N_0}\right\}_{min}$, but both of these requirements cannot hold at the same time. Therefore, there is a trade-off between these two important parameters depending upon the application type.

Transmission schemes can be roughly divided into two regions based on spectral efficiency η: Power limited for $\eta < 2$ and Bandwidth limited for $\eta > 2$. The redundancy needed for coding in the Power limited region is mainly achieved by increasing the bandwidth W while keeping the signal constellation constant. For a binary coding scheme, the maximum coded symbol rate can approach the Nyquist limit of 2W coded−symbols/second, in that case, the maximum transmission rate becomes $R = R_c \times 2W$ for a code rate $R_c \leq 1$. As $\eta = \frac{R}{W}$, attains the value $\eta \leq 2$ bits/s/Hz and reaches its maximum value of 2 for $R_c = 1$, i.e., the uncoded case. Thus, binary

coding schemes can never be used for bandwidth limited systems. Trellis-coded modulation by Gottfried Ungerboeck [7] was the breakthrough in the field of practical coding for bandwidth limited systems. Ungerboeck realized that the needed redundancy for coding can be achieved by increasing the constellation size, M, while keeping W constant, such that $\eta = 2\mathrm{R_c}\log_2 \mathrm{M}$ bits/s/Hz for $\mathrm{R_c} \leq 1$.

The research in the field of channel coding has paved the path for the channel capacity approaching coding schemes. Turbo codes and LDPC codes both belong to a class of iterative a posteriori probability (APP) algorithms. The decoder at the receiver side using these algorithms is also known as *Sum Product algorithm* [5][6] decoder. An excellent survey on the topic of channel capacity has been given by Costello and Forney in [4]. Nevertheless all of these codes were developed by keeping an orthogonal/memoryless modulation assumption in mind.

Discarding the memoryless assumption at the modulation part opens up another dimension for increasing spectral efficiency η. The spectral efficiency, $\eta = \frac{\mathrm{R}}{\mathrm{W}}$, can be increased either by decreasing the W while keeping the transmission rate R constant, or by increasing the transmission rate, R while keeping the M and W same. The former can be achieved by transmitting the signal with correlated symbols at the same rate called *Partial response signaling* [23]. The latter can be achieved by simply increasing the transmission rate R beyond Nyquist rate, called *faster than Nyquist* [3] transmission. Both methods introduce memory to the modulation part which causes an inevitable ISI.

The optimum reception of memory based correlated signal is already known in literature. Forney [8] and Kobayashi [7] proposed the maximum likelihood sequence estimation to detect correlated signals. Both used the Viterbi algorithm which was originally proposed to decode convolution codes. However, an inability of Viterbi algorithm to perform well for larger channel memory is well known. Therefore we have to look for other options for the optimal reception of FTN signals while approaching Shannon's capacity.

Chapter 2

Signals and Systems

Most of the communication systems of the present day work mainly on digital information and use analog waveforms to communicate digital information from one place to another. Some of the examples are digital radio, digital TV, local area network, home electronic devices and mobile telephones.

All of the communication systems are designed keeping some constraints in mind. Parameters like signal power, bandwidth/spectral efficiency, bit error probability and complexity are a few. In this chapter we will talk about the representation of signals, how they are actually transmitted from transmitter and received back at receiver respectively.

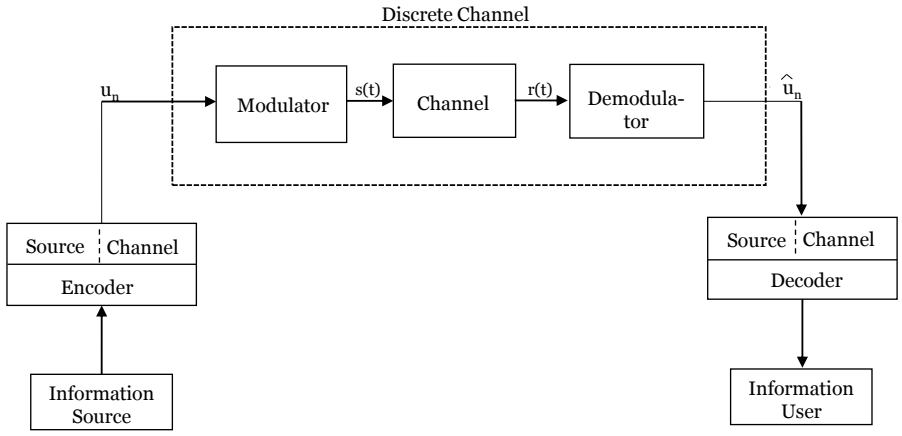

Figure 2.1: Block diagram of digital communication system

The system model shown in Fig. 2.1 gives a brief idea about how the information is communicated between transmitter and receiver. The trans-

mitter and receiver pair are separated by a channel in the Fig. 2.1. The transmitter pass the signal s(t) to the channel which is the medium of separation, some of the examples are optical fiber, wave guide, wireless medium or magnetic strips in CD's. The distorted and noisy signal r(t) is received at the other end called the receiver. The receiver tries to revert back all the changes done by the channel and make a guess about the transmitted signal.

2.1 Transmitter

The main job of the transmitter is to represent the input bit sequence as a sequence of analog waveforms. Actually, the transmitter is fragmented into different parts designed for special tasks. In principle, any information source can be represented by a sequence of binary digits with a source encoder. At the same time a source decoder shall reproduce a replica of information at the receiver side. In this thesis we will presume that the information we dealt with is already in binary form, equiprobable and independent, that is we discard any further discussion about source encoder and source decoder.

The channel encoder and modulator are cascaded in such a way that they reproduce the input binary bits at the output of channel decoder by a suitable modeling of channel waveforms. The classical approach is to consider a memoryless modulation such that an information symbol u_n at time n is mapped to the waveform s(t) and the channel encoder provides the sufficient redundancy to encounter the disturbances caused by the channel. It has been known from a long time now that the memory in the received signal r(t) can be exploited by the channel decoder to make reliable decision about the information bits provided demodulator can extract a sufficient set of statistics about the sent information.

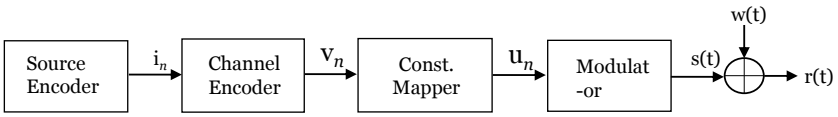

Figure 2.2: Digital transmitter followed by an AWGN channel

Fig. 2.2 shows the typical digital transmitter in the presence of an AWGN channel. Where i_n is a binary information bit sequence coming from a source encoder at a rate $\mathrm{R_b}$ passing through the channel encoder of code rate $\mathrm{R_c}$. The output is an encoded bit sequence v_n at a new rate of $\frac{\mathrm{R_b}}{\mathrm{R_c}}$. These encoded bits are then mapped according to a constellation mapper $\mathcal{A} \in \{\mathrm{a}_0, \mathrm{a}_1, \ldots, \mathrm{a}_{\mathrm{M}-1}\}$ producing a sequence of independent and identically distributed (i.i.d) encoded data symbols u_n. The encoder is chosen such that the output coded symbols are equiprobable and the chosen alphabet $\mathcal{A}$ is balanced, produces random symbols of unit energy, i.e., $\sum_{m=0}^{\mathrm{M}-1} a_m = 0, p(a_m) = \frac{1}{\mathrm{M}}$ and $\sum_{m=0}^{\mathrm{M}-1} \frac{|a_m|^2}{\mathrm{M}} = 1$.

These equiprobable i.i.d data symbols then need to be converted to continuous waveforms before transmitting. From the basics of Fourier series we know that any continuous band-limited function $\mathrm{x}(t)$ ($\int_{-\infty}^{\infty} |\mathrm{x}(t)|^2 \mathrm{d}t < \infty$) can be expanded by an L^2 orthogonal basis $\{\phi_1(t), \phi_2(t), \ldots\}$, such that,

$$\mathrm{x}(t) = \sum_n \mathrm{x}_n \phi_n(t). \tag{2.1}$$

Or in other words, for finite energy series ($\sum_n |\mathrm{x}_n|^2 < \infty$), there always exists an L^2 function $\mathrm{x}(t)$ which satisfies eq. (2.1). This is exactly our requirement at the modulator. A series of real or complex data symbols are required to be mapped into a waveform.

2.1.1 Modulation

Pulse amplitude modulation (PAM) is probably the simplest among all types of modulation schemes. Let $\mathrm{s}(t)$ be a baseband transmission, given by,

$$\mathrm{s}(t) = \sum_n \mathrm{u}_n \mathrm{p}(t - n\mathrm{T_s}). \tag{2.2}$$

The equiprobable i.i.d data symbols u_n (real in case of PAM) are extracted from an alphabet $\mathcal{A} = \{\mathrm{a}_0, \mathrm{a}_1, \ldots, \mathrm{a}_{\mathrm{M}-1}\}$, subsequently mapped to a $\mathrm{T_s}$ spaced basis pulse $\mathrm{p}(t)$. We refer to M as the modulation order and $\mathrm{K} = \log_2 \mathrm{M}$ are the maximum number of bits a data symbol can carry. For example, binary PAM carries one coded bit per data symbol, since $\mathrm{K} = \log_2 2 = 1$. Similarly, 4-PAM carries 2 coded-bits/symbol and 16-PAM carries 4 coded-bits/symbol respectively. The modulation schemes where $\mathrm{K} > 1$ are called multilevel modulation. The symbol rate (or baud rate) of the data transmission is given by $\mathrm{R_s} = \frac{1}{\mathrm{T_s}}$, the baud rate is the maximum number of uncoded/coded data symbols transmitted in one second.

How are we going to decide on the choice of basis pulse $\mathrm{p}(t)$? To answer this question we need to understand the Nyquist Criterion of ISI free transmission explained in the next section.

2.1.2 Demodulation

Let the received baseband signal be $\mathrm{r}(t) = \sum_n \mathrm{u}_n \mathrm{p}(t - n\mathrm{T_s})$, observe that we are ignoring any impairments normally observed between transmitter and receiver at this point of time. To retrieve back the data symbols, $\mathrm{r}(t)$ is passed through a filter with impulse response $\mathrm{q}(t)$ followed by a sampler at a rate $m\mathrm{T_s}$.

The filter $\mathrm{q}(t)$ output is given by,

$$\mathrm{y}(t) = \int_{-\infty}^{\infty} \mathrm{r}(\tau)\mathrm{q}(t-\tau)\mathrm{d}\tau. \tag{2.3}$$

Here, $\mathrm{q}(t)$ is chosen such that $\mathrm{y}(m\mathrm{T_s}) = \mathrm{u}_n$,

$$\begin{aligned}
\mathrm{y}(t) &= \int_{-\infty}^{\infty} \sum_{n=0}^{\infty} \mathrm{u}_n \mathrm{p}(\tau - n\mathrm{T_s})\mathrm{q}(t-\tau)\mathrm{d}\tau, \\
&= \sum_{n=0}^{\infty} \mathrm{u}_n \int_{-\infty}^{\infty} \mathrm{p}(\tau - n\mathrm{T_s})\mathrm{q}(t-\tau)\mathrm{d}\tau, \\
&= \sum_{n=0}^{\infty} \mathrm{u}_n \mathrm{g}(t - n\mathrm{T_s}),
\end{aligned}$$

where, $\mathrm{g}(t) = \mathrm{p}(t) * \mathrm{q}(t) = \int_{-\infty}^{\infty} \mathrm{p}(\tau)\mathrm{q}(t-\tau)\mathrm{d}\tau$, $(*)$ is the convolution operator. Now for perfect reception, i.e., ISI free reception, $\mathrm{y}(m\mathrm{T_s}) = \mathrm{u}_n$ for every sampling interval $t = m\mathrm{T_s}$, which is only possible if the pulse $\mathrm{g}(t)$ satisfies eq. (2.4),

$$\mathrm{g}(m\mathrm{T_s} - n\mathrm{T_s}) = \begin{cases} 1 & n = m \\ 0 & n \neq m. \end{cases} \tag{2.4}$$

The pulses of type defined in eq. (2.4) are known as Nyquist pulses. Any pulse $\mathrm{g}(t)$ is considered as an ideal Nyquist with time interval $\mathrm{T_s}$ if and only if $\mathrm{G}(f) = \mathscr{F}\{\mathrm{g}(t)\}$, ($\mathscr{F}$ = Fourier transform), satisfies the *Nyquist criterion* which is defined as,

$$\frac{1}{\mathrm{T_s}} \sum_{n=-\infty}^{\infty} |\mathrm{G}(f + \frac{n}{\mathrm{T_s}})|\mathrm{rect}(f\mathrm{T_s}) = \mathrm{rect}(f\mathrm{T_s}), \tag{2.5}$$

for,

$$\mathrm{rect}(t) = \begin{cases} 1 & -\frac{1}{2} \leq t \leq \frac{1}{2} \\ 0 & \text{elsewhere.} \end{cases}$$

The Nyquist pulse g(t) which satisfies zero ISI at sampling interval is ought to have valid Nyquist criterion for G(f) in frequency domain and vice versa. From eq. (2.4) and eq. (2.5) we can say that the transmitted and received filter waveforms shall produce an orthonormal effect. Therefore we need to find the set of pulses whose combined effect is orthonormal with the time-shift $\mathrm{T_s}$ to avoid ISI.

The basis pulse filter p(t) and receiver filter q(t) are cascaded to each other to produce an ideal Nyquist pulse. As the receiver filter q(t) must be matched to p(t) to produce an ideal Nyquist pulse effect, it is usually referred to as a *matched filter*. The most important thing here is that the pulse that satisfies the Nyquist criterion should be strictly bandlimited and time limited as well, which is not possible according to a basic principle of mathematics, which says that restriction in one domain causes inevitable extension in another domain. We will focus on strictly bandlimited pulses G(f) and truncate the pulse in time domain, just before transmitting, to fit the latter condition.

From eq. (2.5), rect(fT) is the first theoretical choice for G(f) to satisfy Nyquist criterion. Unfortunately the sharp frequency response of rect(fT) increases the filter order and makes practical implementation very difficult. Therefore other practical choices shall be looked for.

The minimum bandwidth required for a pulse g(t) orthogonal to every time shift $\mathrm{T_s}$ is $\mathrm{W_N} = \frac{1}{2\mathrm{T_s}}$. The actual bandwidth W associated with g(t) is always greater that $\mathrm{W_N}$, $\mathrm{W} > \mathrm{W_N}$ such that G(f)=0 for $-\mathrm{W} < \mathrm{f} < \mathrm{W}$ and $\mathrm{W} = \mathrm{W_N}$ is possible only if G(f)=rect($f\mathrm{T_s}$). Most practical pulses which satisfy the Nyquist criterion have a symmetry in G(f) around W such that; $\mathrm{G(W} + \Delta) = \mathrm{G(W} - \Delta)$[9]. The *Root Raised Cosine* (RRC) is another class of Nyquist pulses which satisfies Nyquist criterion with a roll-off factor β. The name RRC comes from the fact that, the function has a square root raised cosine shape in the frequency domain. In frequency domain the RRC pulses can be given by,

$$|\mathrm{G}(f)|^2 = \begin{cases} \mathrm{T}, & |f| \geq \frac{1-\beta}{2\mathrm{T}} \\ \mathrm{T}\cos^2(\frac{\pi \mathrm{T}}{2\beta}), & \frac{1-\beta}{2\mathrm{T}} < |f| \geq \frac{1+\beta}{2\mathrm{T}} \\ 0, & |f| > \frac{1+\beta}{2\mathrm{T}}. \end{cases} \tag{2.6}$$

The function defined in eq. (2.6) decays with a rate of $\frac{1}{t^3}$ in time domain in comparison to the decay rate of $\frac{1}{t}$ for rect(fT). This fast rate of decay in the time domain makes the frequency response less sharp and hence decreases the order of the filter. This is responsible for the practical implementation of the root raised cosine basis pulse. The practical implementation to satisfy Nyquist criteria consumes $\beta\%$ more bandwidth for the signaling rate $\frac{1}{\mathrm{T_s}}$. Fig. 2.3 shown below represents the root raised cosine pulses in the time domain and frequency domain with different roll-off factors. As the rolloff factor increases the pulse in the time domain decays more quickly but in the frequency domain it utilizes more bandwidth. The rolloff factor $\beta = 0$ represents a sinc pulse.

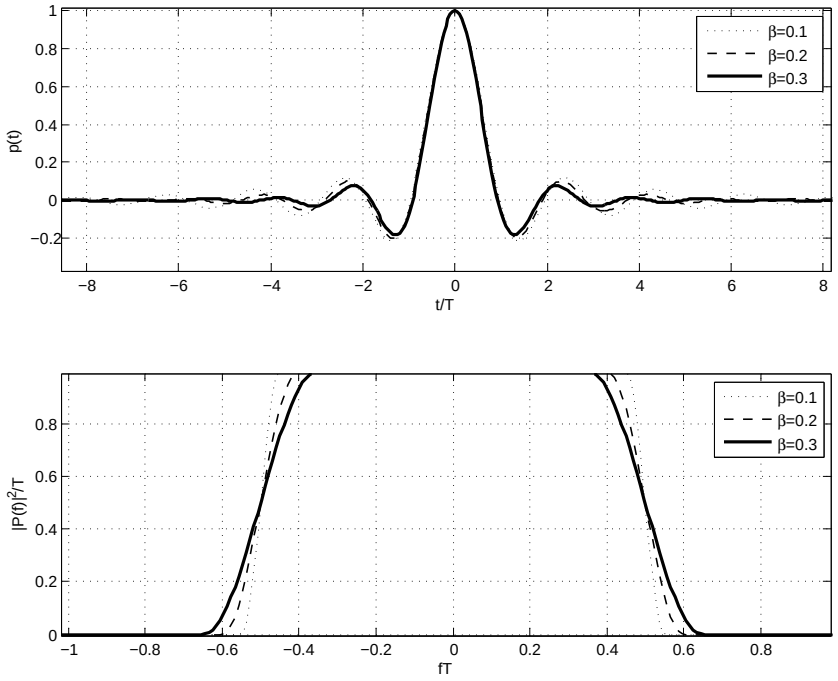

Figure 2.3: Root raised cosine pulses satisfies Nyquist ISI criteria with roll-off factor β

2.1.3 Baseband to Pass-band conversion

Till now we have discussed the ISI free baseband implementation of the transmitted signal. In reality there is an assigned bandwidth associated with the transmission type. For example LTE transmission in Sweden is

centered on the bands of 800/1800/2600 MHz. So, there is a need of up conversion from baseband to the allotted bandwidth before transmission. As the main objective is to shift frequency from $[0, \mathrm{W}]$ to $f_\mathrm{c} - \mathrm{W} \leq f_\mathrm{c} \leq f_\mathrm{c} + \mathrm{W}$, it can be easily done by $\mathrm{s}(t)\exp^{2\pi i f_\mathrm{c} t} \leftrightarrow \mathrm{S}(f - f_\mathrm{c})$ where $\mathrm{S}(f) = \mathscr{F}\{\mathrm{s}(t)\}$.

In practice, the baseband to carrier modulated passband conversion is done as,

$$\begin{aligned} \mathrm{s_P}(t) &= \mathrm{s}(t)[e^{2\pi i f_\mathrm{c} t} + e^{-2\pi i f_\mathrm{c} t}], \\ \mathrm{s_P}(t) &= 2\mathrm{s}(t)\cos(2\pi i f_\mathrm{c} t), \end{aligned}$$

in frequency domain,

$$\mathrm{S_P}(f) = \mathrm{S}(f - f_\mathrm{c}) + \mathrm{S}(f + f_\mathrm{c}).$$

In PAM the baseband signal $\mathrm{S}(f)$ consumes positive bandwidth W but in the passband $\mathrm{S_P}(f)$ covers double than the baseband case i.e. 2W, whereas the number of symbols it carries is same, both in baseband and passband. There is wastage of W in double sided PAM transmission. One solution to this problem is to consider only one side band in the passband signal while transmission, the other band can be easily retrieve, as $\mathrm{S}(f) = \mathrm{S}(-f)$ called single side band PAM. Another solution is to use the quadrature dimension as well. Modulation schemes which use both real and quadrature dimensions are called Quadrature Amplitude Modulation (QAM). In QAM, $\mathrm{s}(t)$ is complex.

The carrier modulated QAM signal can be written as,

$$\mathrm{s_P}(t) = \mathrm{s}(t)e^{2\pi i f_\mathrm{c} t} + \mathrm{s}^*(t)e^{-2\pi i f_\mathrm{c} t},$$

where, $(.)^*$ is the complex conjugate operation. Another way of writing the above equation is,

$$\mathrm{s_P}(t) = 2\Re\left\{\mathrm{s}(t)e^{2\pi i f_\mathrm{c} t}\right\}. \tag{2.7}$$

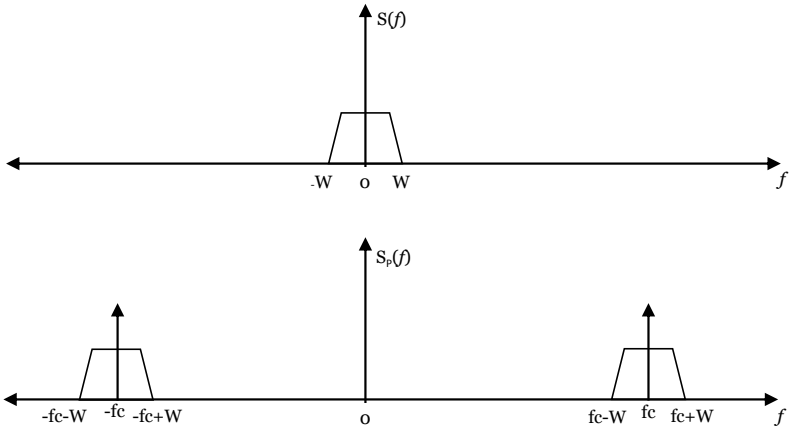

Figure 2.4: Baseband and Passband representation of signal

In QAM the constellation points are complex,
$\mathcal{A} = \{a_0 + ia'_0, a_1 + ia'_1, ..., a_{M-1} + ia'_{M-1}\}$. The constellation points are arranged symmetrically about the origin forming a square grid. Baseband to passband conversion and demodulation processes are all same in PAM and QAM. QAM is nothing but PAM in both the dimensions.

2.1.4 Conservation of Distance

The distance between signal points is a very important parameter used in many applications. The *Minimum Euclidean Distance Receiver* is one of many examples [10]. For basis pulse $p(t)$ with orthonormal shifts, the distance between two baseband signals $u(t) = \sum_n u_n p(t - nT_s)$ and $u'(t) = \sum_n u'_n p(t - nT_s)$ can be found out by,

$$\left(\int_{-\infty}^{\infty} |u(t) - u'(t)|^2 dt\right)^{\frac{1}{2}} = \left(\sum_n |u_n - u'_n|^2\right)^{\frac{1}{2}}. \tag{2.8}$$

Similarly, the distance between passband signals $u_p(t)$ and $u'_p(t)$ can be given by,

$$\begin{aligned}\left(\int_{-\infty}^{\infty} |u_p(t) - u'_p(t)|^2 dt\right)^{\frac{1}{2}} &= \left(\int_{-\infty}^{\infty} |2\Re\left\{u(t)e^{2\pi i f_c t}\right\} - 2\Re\left\{u'(t)e^{2\pi i f_c t}\right\}|^2 dt\right)^{\frac{1}{2}}, \\ &= \left(\int_{-\infty}^{\infty} |2\Re\{[u(t) - u'(t)]e^{2\pi i f_c t}\}|^2 dt\right)^{\frac{1}{2}},\end{aligned}$$

taking out the complex exponential and comparing with eq. (2.8), we get,

$$\left(\int_{-\infty}^{\infty} |\mathrm{u_p}(t) - \mathrm{u'_p}(t)|^2 \mathrm{d}t\right)^{\frac{1}{2}} = 2\left(\sum_n |\mathrm{u}_n - \mathrm{u'}_n|^2\right)^{\frac{1}{2}}. \tag{2.9}$$

By comparing eq. (2.8) and eq. (2.9) we get,

$$\left(\int_{-\infty}^{\infty} |\mathrm{u_p}(t) - \mathrm{u'_p}(t)|^2 \mathrm{d}t\right)^{\frac{1}{2}} = 2\left(\int_{-\infty}^{\infty} |\mathrm{u}(\mathrm{t}) - \mathrm{u'}(\mathrm{t})|^2 \mathrm{d}\mathrm{t}\right)^{\frac{1}{2}}. \tag{2.10}$$

We can see from eq. (2.10) that the distance between signals in baseband and passband form is preserved apart from the scaling factor of 2. This is the reason why we always analyze and investigate in the baseband only and implement the same result for the passband. In this thesis the signals are always baseband limited.

2.2 Memoryless channel model

Till now we have seen how to modulate and demodulate the signal, but we ignored all the limiting factors between transmitter and receiver. Noise is the fundamental limitation to communicate over physical channels. The communication channel that adds white Gaussian noise to the transmitted signal is called AWGN channel.

The AWGN channel model is given by,

$$\mathrm{r}(t) = \mathrm{s}(t) + \mathrm{w}(t). \tag{2.11}$$

In continuous domain at the receiver side, $\mathrm{r}(t)$ is received as ISI free transmitted signal $\mathrm{s}(t)$ with additive Gaussian noise $\mathrm{w}(t)$. In this model we are assuming that attenuation by the channel, time delay and carrier phase distortion have already been taken care off. Noise $\mathrm{w}(t)$ is modeled as a random process, first because it is a priori unknown; secondly because it is known to behave in some statistical way. Particularly, the noise $\mathrm{w}(t)$ has a power spectral density of $\frac{\mathrm{N}_0}{2}$ at all frequencies.

As explained in Section 2.1.2, the received signal $\mathrm{r}(t)$ is passed through a unit energy matched filter and a sampler. At the output of sampler we get,

$$\mathrm{y}(m) = \sum_n \mathrm{u}_n \mathrm{g}\left(\frac{m\mathrm{T_s} - n\mathrm{T_s}}{\mathrm{T_s}}\right) + \mathrm{w}_m.$$

At Each epoch $m\mathrm{T_s}$, the noise w_m is modeled as Gaussian random variable with $\mathcal{N}(0, \frac{N_0}{2})$, i.e., mean $\mu = 0$ and variance $\sigma^2 = \frac{\mathrm{N_0}}{2}$ and data symbols are equiprobable i.i.d. expanded by the Nyquist pulse $\mathrm{g}(t)$. Therefore the discrete model can be rewritten as,

$$\mathbf{y} = \mathbf{u} + \mathbf{w}, \tag{2.12}$$

where, $\mathbf{u}$ and $\mathbf{w}$ are vectors containing data symbols and noise samples respectively.

2.3 Detection of ISI free received signal

After receiving the noise corrupted signal, it is time to make a decision about the transmitted signal. At first glance, making a correct decision from corrupted received signal looks quite ambiguous. But in reality correct decision is made with quite a precision. Note that here we are considering the ISI free case which means that each symbol is corrupted by noise only, whereas there is no effect from the neighboring signals (recall eq. (2.11)).

2.3.1 MAP detector

The MAP detector makes a decision on each of u_n by observing the received sample y_n and mapping the decision to $\hat{\mathrm{u}}_n$. The rule for maximizing the probability of correct decision is to choose $\hat{\mathrm{u}}_n$ to be $\mathrm{a} \in \mathcal{A}$ for which $\mathrm{p}(\mathrm{a}|\mathbf{y})$ is maximized. This rule of maximizing the probability of correct decision is also known as *Maximum a posteriori* (MAP) rule. The MAP rule is given by,

$$\hat{\mathrm{u}}_n = \arg \max_{\mathrm{a}\in\mathcal{A}} \mathrm{p}(\mathrm{a}|\mathbf{y}) \quad (\textbf{MAP rule}), \tag{2.13}$$

since, the noise we considered is white Gaussian noise, therefore eq. (2.13) becomes,

$$\hat{\mathrm{u}}_n = \arg \max_{\mathrm{a}\in\mathcal{A}} \mathrm{p}(\mathrm{a}|\mathrm{y}_n) \quad (\textbf{MAP rule}). \tag{2.14}$$

The $\arg \max_{\mathrm{a}\in\mathcal{A}}$ means the value of argument a that maximizing the function. This rule gives the optimal solution and a receiver that achieves the lowest possible symbol error probability. We can rewrite the posterior probability in terms of a priori probability with the help of identity shown below,

$$\mathrm{p}(\mathrm{a}|\mathrm{y}_n)\mathrm{p}(\mathrm{y}_n) = \mathrm{p}(\mathrm{y}_n|\mathrm{a})\mathrm{p}(\mathrm{a}),$$
$$\mathrm{p}(\mathrm{a}|\mathrm{y}_n) = \frac{\mathrm{p}(\mathrm{y}_n|\mathrm{a})\mathrm{p}(\mathrm{a})}{\mathrm{p}(\mathrm{y}_n)}.$$

Where $\mathrm{p(a)} = \frac{1}{\mathrm{M}} \forall\, a \in \mathcal{A}$, for equiprobable i.i.d. signal constellation. Therefore, the MAP rule can also be written as,

$$\hat{\mathrm{u}}_n = \mathrm{a} \qquad \text{if} \qquad \frac{\mathrm{p}(\mathrm{y}_n|\mathrm{a})\mathrm{p}(\mathrm{a})}{\mathrm{p}(\mathrm{y}_n)} \geq \frac{\mathrm{p}(\mathrm{y}_n|\tilde{\mathrm{a}})\mathrm{p}(\tilde{\mathrm{a}})}{\mathrm{p}(\mathrm{y}_n)}.$$

As $\mathrm{p(a)} = \mathrm{p}(\tilde{\mathrm{a}}) = \frac{1}{\mathrm{M}}\ \forall\ \mathrm{a}, \tilde{\mathrm{a}} \in \mathcal{A}$, we can cancel the terms p(a) and p($\tilde{\mathrm{a}}$) and also p(y_n) from the inequality. Therefore,

$$\hat{\mathrm{u}}_n = \mathrm{a} \qquad \text{if} \qquad p(\mathrm{y}_n|\mathrm{a}) \geq p(\mathrm{y}_n|\tilde{\mathrm{a}}) \qquad \forall\ \mathrm{a}, \tilde{\mathrm{a}} \in \mathcal{A}.$$

Hence with equiprobable i.i.d. symbols, the *MAP* decision rule becomes equivalent to the maximum likelihood decision rule (*ML*).

2.3.2 Minimum Euclidean Distance detector

For an AWGN channel,

$$\mathrm{p}(\mathrm{y}_n|\mathrm{a}) = \mathrm{p_w}(\mathrm{y}_n - \mathrm{a}), \tag{2.15}$$

$\mathrm{p_w}$ is the probability density function (pdf) of Gaussian noise. Hence, the MAP rule for an AWGN channel can be written as,

$$\hat{\mathrm{u}}_n = \mathrm{a} \qquad \text{if} \qquad \mathrm{e}^{\frac{-|\mathrm{y}_n - \mathrm{a}|^2}{\mathrm{N}_0}} \mathrm{p(a)} \geq \mathrm{e}^{\frac{-|\mathrm{y}_n - \tilde{\mathrm{a}}|^2}{\mathrm{N}_0}} \mathrm{p}(\tilde{\mathrm{a}}) \qquad \forall\, \mathrm{a}, \tilde{\mathrm{a}} \in \mathcal{A}. \tag{2.16}$$

By taking **log** on both sides we get,

$$\hat{\mathrm{u}}_n = \mathrm{a} \text{ if } \frac{-|\mathrm{y}_n - \mathrm{a}|^2}{\mathrm{N}_0} + \log\left(\mathrm{p(a)}\right) \geq \frac{-|\mathrm{y}_n - \tilde{\mathrm{a}}|^2}{\mathrm{N}_0} + \log(\mathrm{p}(\tilde{\mathrm{a}}))\ \forall\, \mathrm{a}, \tilde{\mathrm{a}} \in \mathcal{A}.$$

Now, multiply by -1 on both sides of inequality, we then get,

$$\hat{\mathrm{u}}_n = \mathrm{a} \text{ if } \frac{|\mathrm{y}_n - \mathrm{a}|^2}{\mathrm{N}_0} - \log\left(\mathrm{p(a)}\right) \leq \frac{|\mathrm{y}_n - \tilde{\mathrm{a}}|^2}{\mathrm{N}_0} - \log(\mathrm{p}(\tilde{\mathrm{a}}))\ \forall\, \mathrm{a}, \tilde{\mathrm{a}} \in \mathcal{A}.$$

For equiprobable i.i.d. data symbols, we can write,

$$\hat{\mathrm{u}}_n = \mathrm{a} \qquad \text{if} \qquad |\mathrm{y}_n - \mathrm{a}|^2 \leq |\mathrm{y}_n - \tilde{\mathrm{a}}|^2 \qquad \forall\, \mathrm{a}, \tilde{\mathrm{a}} \in \mathcal{A}. \tag{2.17}$$

Therefore, we can say that, *MAP* detector for an AWGN channel is also a *minimum Euclidean distance* detector.

2.3.3 Probability of error for memoryless AWGN channel

The probability of error for an AWGN channel is bounded by,

$$\mathrm{P_e} = (\mathrm{M}-1)\,\mathrm{Q}\left[\frac{\mathrm{d_{min}}}{2\sigma}\right], \tag{2.18}$$

where M is modulation order, $\mathrm{d_{min}}$ is minimum Euclidean distance and $\sigma = \sqrt{\frac{\mathrm{N_0}}{2}}$ is the standard deviation of the discrete-time noise.

2.4 Channel with memory

The links between earth and deep space are often modeled as instances of the discrete memoryless channel (DMC) which was discussed in the previous section, whereas communication on earth or below ionosphere, due to multipath components apart from additive interference also suffers interference of multiplicative nature. Therefore the signal model given in eq. (2.11) doesn't hold anymore.

The received signal $\mathrm{r}(t)$ in the presence of channel $\mathrm{h}(t)$ can be written as,

$$\mathrm{r}(t) = \mathrm{h}(t) * \mathrm{s}(t) + \mathrm{w}(t), \tag{2.19}$$

where channel is modeled as a finite impulse response $\mathrm{h}(t)$ of length L, such that, $\mathrm{h}(t)$ takes non-zero values for only $0 < t < (\mathrm{L}-1)\mathrm{T_s}$. By substituting $\mathrm{s(t)} = \sum_{\mathrm{n}} \mathrm{u_n p(t - nT_s)}$ in eq. (2.19), gives,

$$\begin{aligned}\mathrm{r}(t) &= \mathrm{h}(t) * \sum_{n} \mathrm{u_n p}(t - n\mathrm{T_s}) + \mathrm{w}(t),\\ &= \sum_{n} \mathrm{u}_n \left(\mathrm{h}(t) * \mathrm{p}(t - n\mathrm{T_s})\right) + \mathrm{w}(t).\end{aligned}$$

After passing $\mathrm{r}(t)$ through a match filter $\mathrm{q}(t) = \mathrm{p}^*(-t)$ and recalling the demodulation section, we get,

$$\mathrm{y}(t) = \sum_{n} \mathrm{u}_n \left(\mathrm{h}(t) * \mathrm{g}(t - n\mathrm{T_s})\right) + \mathrm{n}(t) \qquad \{\mathrm{g}(t) = \mathrm{NyquistPulse}\}, \tag{2.20}$$

where $\mathrm{n}(t)$=$\mathrm{w}(t)$*$\mathrm{q}(t)$ and for a unit energy $\mathrm{q}(t)$, $\mathbb{E}\{\mathrm{n}[l]\mathrm{n}^*[m]\} = \sigma_{\mathrm{n}}^2\delta[l-m]$. For a finite memory L and orthogonal basis function $\phi(t)$,
$\mathrm{h}(t) = \sum_{l=0}^{\mathrm{L}} \mathrm{h}_l\phi(t - l\mathrm{T_s})$ and $\mathrm{n}(t) = \sum_m \mathrm{n}_m\phi(t - m\mathrm{T_s})$, the eq. (2.20) be-

comes,

$$\mathrm{y}(t) = \sum_n \mathrm{u}_n \left(\sum_{l=0}^{\mathrm{L}} \mathrm{h}_l \phi(t - l\mathrm{T_s}) * \mathrm{g}(t - n\mathrm{T_s}) \right) + \sum_m \mathrm{n}_m \phi(t - m\mathrm{T_s}),$$

$$\mathrm{y}(m\mathrm{T_s}) = \sum_{l=0}^{\mathrm{L}} \mathrm{h}_l \mathrm{u}_{m-l} + \mathrm{n}_m,$$

$$\mathrm{y}_m = \sum_{l=0}^{\mathrm{L}} \mathrm{h}_l \mathrm{u}_{m-l} + \mathrm{n}_m,$$

here, y_m is the set of sufficient statistics for estimating the sent symbols u_m. In vector form,

$$\mathbf{y} = \mathrm{H}\mathbf{u} + \mathbf{n}. \tag{2.21}$$

In eq. (2.21), matrix H is the Toeplitz matrix of size $(\mathrm{N} + \mathrm{L}) \times \mathrm{N}$, $\mathbf{u}$ is an $(\mathrm{N} \times 1)$ signal vector and $\mathbf{n}$ is an $(\mathrm{N} \times 1)$ vector containing Gaussian noise samples. Eq. (2.21) is the discrete AWGN time model for channels with memory. At every sampling interval there is interference from neighboring samples as well apart from the noise. Also, $\mathbf{y}$ forms a set of sufficient statistics for estimating $\mathbf{u}$. The matched filter considered in the above derivation was only matched with the basis pulse p(t) such that $\mathrm{q(t)} = \mathrm{p}^*(-\mathrm{t})$ not with the combination of basis pulse p(t) and channel h(t) where it would have been $\mathrm{q(t)} = \mathrm{c}^*(-\mathrm{t})$ for $\mathrm{c(t)} = \mathrm{h(t)} * \mathrm{p(t)}$. With the approach we adopted the noise samples remained white.

2.5 Detection of received signal with ISI

2.5.1 MLSE decoding

The *Maximum-Likelihood sequence estimation* (MLSE) rule is given by,

$$\hat{\mathbf{u}} = \arg \max_{\mathbf{a}} \mathrm{P}(\mathrm{r}(t)|\mathbf{a}) \ \forall \ \mathbf{a} \in \mathcal{A}^{\mathrm{N}}. \tag{2.22}$$

Like before, it can be easily shown that maximizing $\mathrm{P}(\mathrm{r}(t)|\mathbf{a})$ is equivalent to minimizing the Euclidean distance. Therefore,

$$\hat{\mathbf{u}} = \arg \max_{\mathbf{a}} \left(\int_{-\infty}^{\infty} |\mathrm{r}(t) - \mathrm{h}(t) * \mathrm{s}(t)|^2 \mathrm{d}t \right) \ \forall \ \mathbf{a} \in \mathcal{A}^{\mathrm{N}}, \tag{2.23}$$

in the discrete domain, i.e., after matched filter and sampling, it can be written as,

$$\hat{\mathbf{u}} = \arg \max_{\mathrm{a}} \left(\sum_{n=0}^{\mathrm{N+L+1}} |\mathrm{y}_n - \sum_{l=0}^{\mathrm{L}} \mathrm{h}_l \mathrm{a}_{n-l}|^2 \} \right) \ \forall \ \mathrm{a} \in \mathcal{A}. \tag{2.24}$$

In eq. (2.23), $\hat{\mathbf{u}}$ and $\mathbf{a}$ are the entire estimated sequence and trial sequence respectively. Since the decision has been made on the entire sequence the decision rule is known as Maximum-likelihood sequence estimation. For a modulation order M there can be $\mathrm{M^N}$ different trial sequences ($\mathbf{a}$) which makes the computational complexity of order $\mathrm{O(M^N)}$. Fortunately the *Viterbi algorithm* can be used for such ISI sequence estimation problem with a reduced complexity from the order of exponential in N to exponential in the channel memory L i.e., $\mathrm{O(NM^L)}$. For the first time Forney introduces the application of VA in the reception of ISI signals of the form eq. (2.21), later Ungerboeck proved the same thing in the presence of colored noise [8][11]. In the Viterbi algorithm the minimum distance sequence is equivalent to the recursively finding the highest accumulated path metric at each trellis stage.

Although complexity has been decreased, still it needs a lot of computations for either a large cardinality of the alphabet M, or significantly larger memory in the channel part, theoretically which is infinite in length. There are other sub-optimal choices available such as the linear *Zero-forcing* equalizer and the *MMSE* equalizer and non-linear *feedback* equalizer [25]. These are relatively less complex and can be cascaded with the optimal channel decoder. Since 1993 [24], important advances have been made in the field of turbo equalization. One of such examples is [12] where a MAP based MMSE equalizer have been developed. A joint iterative MAP equalization cascaded with MAP decoding is the state of art technology of present time, which impressively approached the Shannon's capacity limit. We have used an iterative SISO *Minimum Mean Squared Error equalization* using a priori information cascaded with an *LDPC decoder* to improve on the overall performance of the *faster than Nyquist* system.

2.5.2 MAP decoding

The MAP decoding of eq. (2.21) type of signal model is considered here. The MAP sequence decoder gives,

$$\hat{\mathrm{a}} = \arg\max_{\mathbf{a}} \mathrm{P}(\mathbf{a}|\mathbf{y}) = \arg\max_{\mathbf{a}} \mathrm{P}(\mathbf{y}|\mathbf{a})\mathrm{P}(\mathbf{a}).$$

For independent data symbols the a priori probability is $\mathrm{P}(\mathbf{a}) = \prod_n \mathrm{p}(\mathrm{y}_n|\mathbf{a})$ and $\mathrm{P}(\mathbf{y}|\mathbf{a}) = \prod_n \mathrm{p}(\mathrm{y}_n|\mathbf{a})$, where,

$\prod_n \mathrm{p}(\mathrm{y}_n|\mathbf{a}) = \mathrm{e}^{\frac{-1}{\mathrm{N}_0}||\mathrm{y}_n - \sum_{l=0}^{\mathrm{L}} \mathrm{h}_l \mathrm{a}_{n-l}||^2}$ (Note: The constant term has been ignored here).

Therefore, $\hat{\mathrm{a}}_n = \arg\max_{\mathrm{a}_n} \prod_n \mathrm{p}_{\mathrm{y}|\mathrm{a}}(\mathrm{y}_n|\mathbf{a}) \prod_n \mathrm{p}(\mathrm{a}_n)$ provides the MAP decoder output at each epoch. Also it provides soft output for each symbol in terms of Log APP (a posteriori probability) ratios,

$$\mathrm{L}(\mathrm{a}_n|\mathbf{y}) \triangleq \log \frac{\mathrm{p}(\mathrm{a}_n = 0|\mathbf{y})}{\mathrm{p}(\mathrm{a}_n = 1|\mathbf{y})} = \log \frac{\sum_{\mathrm{a}:\mathrm{a}_n=0} \mathrm{p}(\mathbf{a}|\mathbf{y})}{\sum_{\mathrm{a}:\mathrm{a}_n=1} \mathrm{p}(\mathbf{a}|\mathbf{y})}. \tag{2.25}$$

The eq. (2.25) can be divided into two parts, for $n \neq n'$,

$$\mathrm{L}(\mathrm{a}_n|\mathbf{y}) = \log \frac{\sum_{\mathrm{a}:\mathrm{a}_n=0} \mathrm{P}(\mathbf{y}|\mathbf{a})\mathrm{P}(\mathbf{a})}{\sum_{\mathrm{a}:\mathrm{a}_n=1} \mathrm{P}(\mathbf{y}|\mathbf{a})\mathrm{P}(\mathbf{a})} = \log \frac{\sum_{\mathrm{a}:\mathrm{a}_n=0} \mathrm{P}(\mathbf{y}|\mathbf{a}) \prod_{n'} \mathrm{p}(a'_n)}{\sum_{\mathrm{a}:\mathrm{a}_n=1} \mathrm{P}(\mathbf{y}|\mathbf{a}) \prod_{n'} \mathrm{p}(a'_n)} + \mathrm{L}(\mathrm{a}_n). \tag{2.26}$$

The left hand side of the sum in eq. (2.26) represent the information about a_n contained in $\mathbf{y}$ (the channel output) and in symbols $\mathrm{a}_{n'}$ other than a_n itself. If we could somehow manage to get these $\mathrm{a}_{n'}$ information prior to the calculation, we can leverage this information to reduce the ISI. This is the approach taken by the MMSE based soft equalizer. The Turbo MMSE soft equalizer takes the extrinsic information (a priori information) from the output of channel decoder and provides the soft outputs from equalizer to the channel decoder.

Chapter 3

Faster than Nyquist signaling, Background and Motivation

For ISI free transmission over an AWGN channel of baseband bandwidth W, it requires the received samples at the receiver side $\mathrm{y}(m\mathrm{T_s}) = \mathrm{u}_m + \mathrm{w}_m \ \forall\, m \in \mathbb{N}$, with a baud rate of $\frac{1}{\mathrm{T_s}}$. The positive Nyquist baseband bandwidth associated with the signal interval $\mathrm{T_s}$ is $\mathrm{W_N} = \frac{1}{2\mathrm{T_s}}$, while the actual baseband bandwidth W shall hold the inequality, $\mathrm{W} \geq \mathrm{W_N}$, to satisfy Nyquist criterion, $\mathrm{W} = \mathrm{W_N}$ for sinc pulses only. If we increase the baud rate $\frac{1}{\tau\mathrm{T_s}}$ $(\tau < 1)$ without increasing the bandwidth W such that the inequality $\mathrm{W} \geq \mathrm{W_N}$ doesn't hold anymore, then there will be an inevitable ISI at the receiver side. This method of transmitting the signal sequence at a baud rate $\frac{1}{\tau\mathrm{T_s}}$ $(\tau < 1)$ without increasing the required bandwidth to avoid ISI is called faster than Nyquist signaling. The faster than Nyquist signaling is also known by the acronym *FTN* signaling.

3.1 FTN signals

The transmitted FTN signal sequence is formed by,

$$\mathrm{s}(t) = \sum_{k=0}^{\infty} \mathrm{u}_k \mathrm{p}(t - k\tau\mathrm{T_s}) \qquad \tau \leq 1,$$

where u_k is a sequence of equiprobable i.i.d. data symbols randomly drawn from an alphabet $\mathcal{A}$. The basis pulse $\mathrm{p}(t)$ is an unit energy pulse and orthogonal for every symbol time shift $\mathrm{T_s}$. Now there exists an integer n such that $\int \mathrm{p}(t)\mathrm{p}(t - n\tau\mathrm{T_s}) \neq 0$. Therefore, there is an inevitable ISI with a baud rate of $\frac{1}{\tau\mathrm{T_s}}$ also known as the FTN signaling rate.

Fig. 3.1 illustrates this phenomenon of losing orthogonality for $\tau = 0.8$ in comparison to the Nyquist case with $\tau = 1$. There we took symbols {+1,-1,+1,-1} and modulated this symbol sequence with a RRC pulse forming a

signal sequence of type s(t).

The concept of faster than Nyquist signaling was first put forth by James Mazo in 1975 [3], for binary information carried by sinc pulses. He accelerated the sinc pulses with a rate $\frac{1}{\tau}$ and discovered that the minimum Euclidean distance d^2_{min} does not alter for $0.802 \leq \tau$. It was a surprising result that could carry at maximum $\frac{1}{0.802} \approx 25\%$ more bits in the same bandwidth without increasing the symbol error probability. In FTN the signal is sent every τT_s seconds in comparison to every T_s seconds in the Nyquist case and as a result of this an inevitable ISI occurs. The cost of increased data rate has to be paid off as complexity of FTN system. The complexity lies at the receiver side where the receiver has to take care of the additional ISI as well.

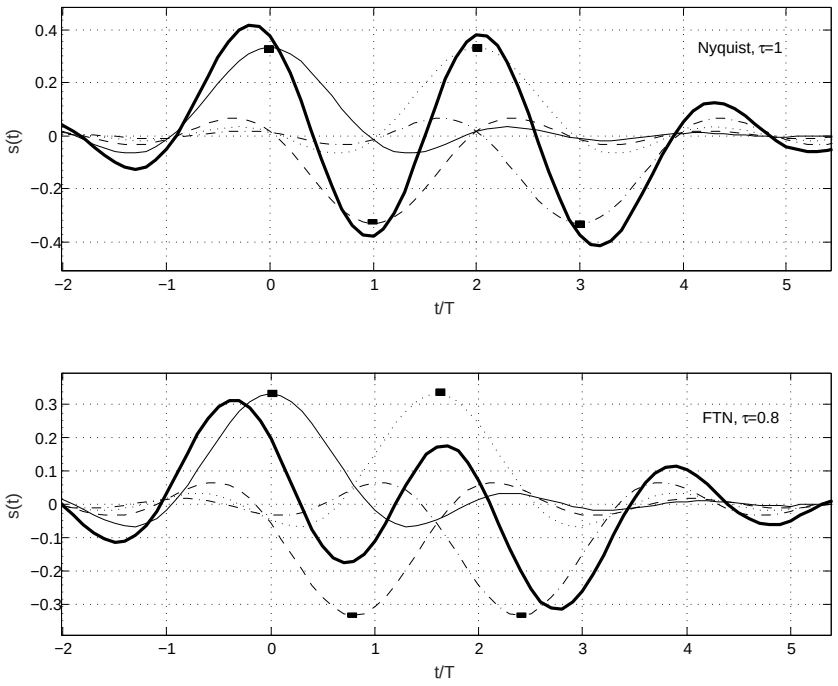

Figure 3.1: Illustration of FTN signaling

Research in the field of FTN after Mazo continued on the minimum distance computations in [13],[14], while some considered it not very promising [17]. In 2003, Liveris and Georghiades investigated the structures of error events for binary FTN and used iterative equalization, turbo decoding and constrained coding techniques to gain more data rates [18]. Later, Rusek and Anderson investigated the information rates related with FTN and they

proved that in many cases the information rates in FTN increases in comparison to the Nyquist case. The increase is due to the excess bandwidth roll off factor β, a smoothing factor to satisfy Nyquist criterion [19], [20]. The less complex M-BCJR algorithm has been investigated in [21] for FTN receivers. Constrained capacities for FTN systems were derived in [22] and they proved that FTN achieves higher capacities than the Nyquist based orthogonal modulation schemes with an excess bandwidth to satisfy Nyquist criterion. Also multidimensional FTN was proposed in [23], where FTN was extended to the frequency domain as well.

In the next section, we derive the discrete AWGN mathematical model for faster than Nyquist signaling. We will take a unit energy pulse and modulate the data symbols at a rate faster than the admissible Nyquist rate for zero ISI.

3.2 FTN system model

In this section we will derive the basic mathematical model for FTN systems. This model will be used in the next chapter to investigate FTN signaling for LTE-uplink type system models. A block diagram of system model for the FTN signaling is represented in Fig. 3.2, shown below.

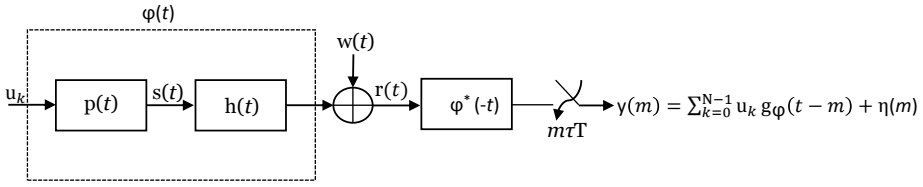

Figure 3.2: System model for FTN signaling

The equiprobable i.i.d. coded/uncoded data symbols u_k drawn from an alphabet $\mathcal{A}$ are modulated with a pulse $\mathrm{p}(t)$ with symbol time $\tau \mathrm{T_s}$ forming a transmitted FTN signal sequence $\mathrm{s}(t)$ which is limited to bandwidth W. $\mathrm{s}(t)$ can be written as,

$$\mathrm{s}(t) = \sum_{k=0}^{\infty} \mathrm{u}_k \mathrm{p}(t - k\tau \mathrm{T_s}), \qquad \tau < 1. \tag{3.1}$$

Now the channel which has been modeled as finite impulse response $\mathrm{h}(t)$ such that $\mathrm{H}(f)=\mathscr{F}\{\mathrm{h}(t)\}$ and bandlimited to W, $\mathrm{H}(f)$ will act as a low pass filter for transmitted signal $\mathrm{u}(t)$ such that $\mathrm{P}(f)\mathrm{H}(f) = \mathrm{P}(f)$. The

transmitted signal $\mathrm{s}(t)$ after passing through a channel of impulse response $\mathrm{h}(t)$ and an AWGN channel is given by,

$$\begin{aligned}\mathrm{r}(t) &= \sum_{k=0}^{\infty} \mathrm{u}_k \mathrm{p}(t - k\tau \mathrm{T_s}) * \mathrm{h}(t) + \mathrm{w}(t),\\ &= \int_{-\infty}^{\infty} \left(\sum_{l=0}^{\mathrm{L}} \mathrm{h}_l \phi(\hat{\tau} - l\mathrm{T_s}) \sum_{k=0}^{\infty} \mathrm{u}_k \mathrm{p}(t - k\tau \mathrm{T_s} - \hat{\tau}) \right) \mathrm{d}\hat{\tau} + \mathrm{w}(t),\\ &= \sum_{k=0}^{\infty} \sum_{l=0}^{\mathrm{L}} \mathrm{u}_k \mathrm{h}_l \mathrm{p}(t - k\tau \mathrm{T_s} - l\mathrm{T_s}) + \mathrm{w}(t), \text{ for } \phi(t) * \mathrm{p}(t) = \mathrm{p}(t),\end{aligned}$$

we can write it like,

$$\mathrm{r}(t) = \sum_{k=0}^{\infty} \mathrm{u_k} \varphi(t - k\tau \mathrm{T_s}) + \mathrm{w}(t), \quad \text{for} \quad \varphi(t) = \sum_{l=0}^{\mathrm{L}} \mathrm{h}_l \mathrm{p}(t - l\mathrm{T_s}). \tag{3.2}$$

Eq. (3.2) represents the received signal sequence $\mathrm{r}(t)$. The received signal $\mathrm{r}(t)$ can be viewed as the sequence of data symbols u_k linearly modulated with a pulse $\varphi(t)$ at a rate of $\frac{1}{\tau \mathrm{T_s}}$ in the presence of an AWGN channel. Now at the receiver side, as already seen in chapter 2, there exists a matched filter to $\varphi(t)$ followed by a sampler. The output of sampler provides a set of sufficient statistics to estimate $\mathrm{u_k}$.

The matched filter output is given by,

$$\mathrm{y}(t) = \int_{-\infty}^{\infty} \mathrm{r}(\hat{\tau}) \varphi^*(-t - \hat{\tau}) \mathrm{d}\hat{\tau}. \tag{3.3}$$

Sampling eq. (3.3) by a sampler at rate $\mathrm{m}\tau \mathrm{T_s}$, provides the below output,

$$\mathrm{y}(m) = \sum_{k=0}^{\mathrm{N}-1} \mathrm{u}_k \mathrm{g}_\varphi(k - m) + \eta(m), \tag{3.4}$$

where $\mathrm{g}_\varphi(t) = \varphi(t) * \varphi^*(-t)$, means that g_φ denotes the $\tau \mathrm{T_s}$ sampled autocorrelation of function $\varphi(t)$. Let's derive g_φ for the received signal sequence $\mathrm{r}(t)$ represented in eq (3.2).

$$\begin{aligned}\mathrm{g}_\varphi(m) &= \int_{-\infty}^{\infty} \varphi(t + m\tau \mathrm{T_s}) \varphi(t) \mathrm{d}t,\\ &= \int_{-\infty}^{\infty} \sum_{m=0}^{L} \sum_{n=0}^{L} \mathrm{h}_m \mathrm{h}_n \mathrm{p}(t - l\mathrm{T_s} + m\tau \mathrm{T_s}) \mathrm{p}(t - n\mathrm{T_s}),\\ &= \sum_{m=0}^{L} \sum_{n=0}^{L} \mathrm{h}_m \mathrm{h}_n \mathrm{g}\left(m + \frac{n}{\tau} - \frac{l}{\tau} \right), \text{ for } \mathrm{g}(t) = \mathrm{p}(t) * \mathrm{p}^*(-t).\end{aligned}$$

Eq (3.4) is also known as *Ungerboeck observation Model* with colored noise samples [11], the variance of noise samples can be written as $\mathbb{E}\{\eta(l)\eta^*(m)\} = \frac{\mathrm{N}_0}{2}\mathrm{g}_\varphi(l-m)$.

Matrix notation

In matrix notation eq. (3.4) can be written as,

$$\mathbf{y} = \mathrm{G}\mathbf{u} + \boldsymbol{\eta}, \tag{3.5}$$

where $\mathbf{y}, \mathbf{u}$ and $\boldsymbol{\eta}$ are vectors of length $\mathrm{N} \times 1$ and G is an $\mathrm{N} \times \mathrm{N}$ Toeplitz matrix containing $\{\mathrm{g}_\varphi[0], \mathrm{g}_\varphi[1], .., \mathrm{g}_\varphi[\mathrm{N}-1]\}$. As many algorithms require the noise to be statistically independent, therefore the Ungerboeck observation Model is not valid as it contained the colored noise samples. The White Noise model is also known as the *Forney Model* [8]. The Forney model can be derived by passing the output of eq (3.4) through a whitening filter. It can be given as,

$$\mathrm{x}_n = \sum_{m=0}^{\mathrm{N}-1} \mathrm{f}(n-m)\mathrm{u}_m + \mathrm{w}_n, \tag{3.6}$$

where $\mathrm{f}(n)$ is a causal ISI sequence such that $\mathrm{f}(n) * \mathrm{f}^*(-n) = \mathrm{g}_\varphi(n)$ and w_n is white Gaussian noise with variance $\mathbb{E}\{w(l)w^*(m)\} = \mathrm{g}_\varphi(0)\frac{N_0}{2}\delta(l-m)$ [28].

Chapter 4

FTN implementation on an LTE-uplink like system model

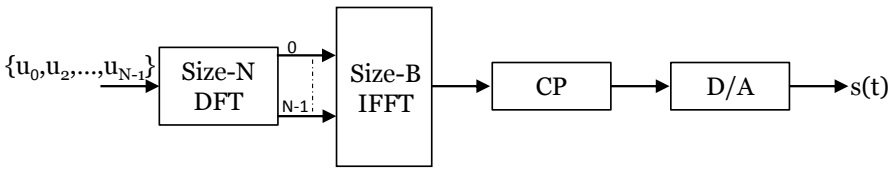

Figure 4.1: Typical LTE-uplink transmitter

A typical LTE-uplink transmitter is shown in Fig. 4.1. The block diagram looks like an OFDM transmitter except for the DFT part and is also known as OFDM based DFT precoded transmitter. A block of size N modulated (coded or uncoded) symbols from an alphabet $\mathcal{A}$ pass through a DFT. The DFT converts the symbols into the frequency domain, where they are mapped to the assigned subcarriers. As frequency mapping depends only upon the size-N DFT block therefore the size of N impacts the transmitted signal bandwidth directly. The frequency mapped symbols are then returned to the time domain by a size-B inverse DFT block such that B>N. The DFT followed by IDFT, provides the signal with the properties of 'single carrier' transmission. The cyclic prefix (CP) is added to each time domain block comes out of the IDFT. The CP should be at least the length of channel memory, $L_{cp} \geq L$ to completely overcome the channel impairments. Practically it is done by copying the last L_{cp} samples to the beginning of the block of size B. At last a D/A conversion is done before transmitting

the signal. If f_s is the sampling frequency of the D/A conversion then the bandwidth of the transmitted signal becomes $W = \frac{N}{B} \times f_s$.

The receiver reverts the changes done by the transmitter and channel on the transmitted block and tries to estimate the transmitted symbols by observing the received signal sequence. A typical LTE receiver consists of an A/D conversion, a size-B DFT, frequency domain equalization and finally a size-N IDFT. In practice, the LTE-uplink uses a turbo encoder to encode the transmitted signal, the turbo encoder consists of a parallel concatenated convolutional code (PCCC) with two recursive convolutional coders and an interleaver. It uses a soft-input/soft-output turbo decoder [25] to decode the received signal. In this thesis, we have used an LDPC encoder at the transmitter side and an iterative SISO MMSE equalizer cascaded with an LDPC decoder at the receiver end.

The rest of the chapter is divided into two main parts. Implementation of faster than Nyquist on LTE-uplink like system models for the uncoded and coded case, respectively.

4.1 Uncoded FTN and its detection

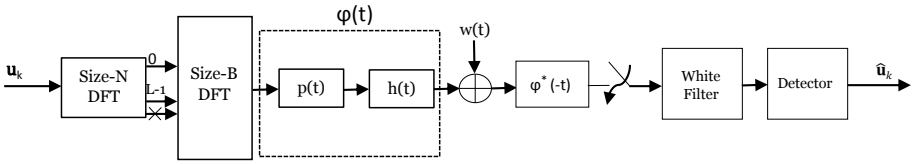

Figure 4.2: Uncoded FTN signaling system model

The transmitter for the baseband single carrier faster than Nyquist signaling is shown in Fig. 4.2. Here we have taken a different approach than the conventional FTN system explained in the previous chapter. The equiprobable i.i.d data symbols sequence $\mathbf{u} = [u_0, u_1, \ldots, u_{N-1}]$ of length N, is drawn from an alphabet $\mathcal{A}$. A DFT operation is performed on this data block $\mathbf{u}$, to convert it into frequency domain followed by a higher order IFFT operation such that only L frequency domain data samples are forwarded, L<N. By eliminating N-L frequency samples increases the data rate by $\frac{N-L}{N}\%$ than

the conventional Nyquist case or it can be interpreted as consuming $\frac{\mathrm{N\text{-}L}}{\mathrm{L}}\%$ less bandwidth to send same amount of data at the expense of inducing unavoidable intersymbol interference. After IFFT operation, digital to analog conversion is performed on the sequence to yield a transmit baseband signal.

Let $\mathbf{s}$ be an B×1 complex vector after IFFT such that $\mathbf{s} = \mathrm{F}\mathbf{u}$, where F is an B×N matrix responsible for DFT operation, N-L frequency components deletion followed by an IFFT operation. Let us derive an expression for the matrix F.

Let $\mathrm{F_B}$ be the Fourier matrix of size B×B defined as,

$$[\mathrm{F_B}]_{kl} = \frac{1}{\sqrt{\mathrm{B}}} \mathrm{e}^{-\mathrm{i}\frac{2\pi}{\mathrm{B}}(k-1)(l-1)};\ 1 \leq k, l \leq \mathrm{B}, \tag{4.1}$$

let Z be a matrix of size B×N defined as,

$$\mathrm{Z} = \begin{pmatrix} \mathrm{I_L} & 0_{\mathrm{L\times N-L}} \\ 0_{\mathrm{B-L\times N}} \end{pmatrix} \quad \text{for} \ \ \mathrm{L} < \mathrm{N} < \mathrm{B}, \tag{4.2}$$

then, F is given by,

$$\mathrm{F} = \frac{\mathrm{N}}{\mathrm{L}} \mathrm{F_B^H Z F_N}. \tag{4.3}$$

Where, subscript $(.)^{\mathrm{H}}$ is the Hermitian transpose, $\mathrm{I_L}$ is an identity matrix of size L×L and 0_{L} is a square matrix of size L×L containing all zeros. Deletion of N-L frequency points decreases the rank of the matrix F to L in comparison to Nyquist case of rank N matrix. The loss of rank is due to deletion of N-L independent rows from the DFT matrix can also be viewed as a loss of orthogonality. Therefore the setup explained above can also be viewed as FTN.

The FTN data sequence $\mathbf{s}$ then pass through a channel and finally received at the other end. As usual, matched filter followed by a sampler at the rate $\mathrm{m}\tau\mathrm{T}$. We considered Forney model, i.e., a whitening filter cascaded after the sampler. To extract back the data symbols, we needed to make decision on the received symbols at each epoch. We have considered the *sphere decoder* for this purpose.

4.1.1 MLSE based sphere decoder

The input sequence $\mathbf{y}$ to the decoder can be written as,

$$\mathbf{y} = \mathrm{H}\mathbf{u} + \mathbf{w}, \tag{4.4}$$

where $H = DF$ is an $B \times N$ matrix, D is an $B \times B$ channel matrix, $\mathbf{y}$ is the received vector of size $B \times 1$ and w is an $B \times 1$ vector, $w = [w_1, w_2, ..., w_{B-1}]^T$ consists of complex white Gaussian noise samples such that each of the real and complex part follow $w_m \in \mathcal{N}(0, \frac{N_0}{2})$. The channel matrix D represents the combined effect by the medium between transmitter and receiver. We considered an assumption that at the receiver side we have full knowledge of the channel, practically which can be easily done by the pilot signals.

The MLSE rule given in eq. (2.23) can be written here as,

$$\hat{\mathbf{u}} = \arg\min_{\tilde{\mathbf{u}}} \left\{ |\mathbf{y} - H\tilde{\mathbf{u}}|^2 \right\}, \tag{4.5}$$

where $\hat{\mathbf{u}}$ and $\tilde{\mathbf{u}}$ are the estimated and trial sequences respectively. For a modulation alphabet of size M, the complexity of eq. (4.5) is of order $O(M^N)$. We used a sphere decoder with relatively less complexity for estimating the sequence $\mathbf{u}$ [26].

Sphere decoding algorithm

The sphere decoding algorithm involves the search only over those lattice points that lie in the sphere of distance d from the received signal $\mathbf{y}$. Therefore complexity of the algorithm depends upon the search radius d. The algorithm involves the QR decomposition of the matrix $H_{B \times N}$, such that,

$$H = Q \begin{bmatrix} R \\ 0_{B-N \times N} \end{bmatrix}, \tag{4.6}$$

where, $Q = [Q_1\ Q_2]$ is an $B \times B$ orthogonal matrix with Q_1 and Q_2 representing first B and last N-B orthonormal columns and R is an $N \times N$ upper triangular matrix. Now for a distance d, a point $H\mathbf{u}$ lies inside the sphere centered around $\mathbf{y}$ if and only if,

$$d^2 \geq ||\mathbf{y} - H\mathbf{u}||^2.$$

By substituting H from eq. (4.6), we get,

$$d^2 \geq \left|\left| \mathbf{y} - [Q_1 \quad Q_2] \begin{bmatrix} R \\ 0 \end{bmatrix} \mathbf{u} \right|\right|^2 = \left|\left| \begin{bmatrix} Q_1^* \\ Q_2^* \end{bmatrix} \mathbf{y} - \begin{bmatrix} R \\ 0 \end{bmatrix} \mathbf{u} \right|\right|^2 = ||Q_1^*\mathbf{y} - R\mathbf{u}||^2 + ||Q_2^*\mathbf{y}||^2,$$

we can write,

$$d^2 - ||Q_2^*\mathbf{y}||^2 \geq ||Q_1^*\mathbf{y} - R\mathbf{u}||^2. \tag{4.7}$$

Let $\mathrm{d}'^2 = \mathrm{d}^2 - ||\mathrm{Q}_2^*\mathbf{y}||^2$ and $\mathbf{x} = \mathrm{Q}_1^*\mathbf{y}$, rewriting eq. (4.7),

$$\mathrm{d}'^2 \geq ||\mathbf{x} - \mathrm{R}\mathbf{u}||^2,$$

$$\mathrm{d}'^2 \geq \sum_{i=1}^{\mathrm{m}} \left(\mathrm{x}_i - \sum_{j=1}^{\mathrm{m}} \mathrm{r}_{i,j}\mathrm{u}_j \right)^2, \tag{4.8}$$

where $\mathrm{r}_{i,j}$ denotes the (i,j) entries from the upper triangular matrix R. Due to the upper triangular matrix R, we can expand the eq. (4.8) as,

$$\mathrm{d}'^2 \geq (\mathrm{x}_m - \mathrm{r}_{m,m}\mathrm{u}_m)^2 + (\mathrm{x}_{m-1} - \mathrm{r}_{m-1,m}\mathrm{u}_m - \mathrm{r}_{m-1,m-1}\mathrm{u}_{m-1})^2 + \ldots. \tag{4.9}$$

The first term on the right side of equality depends only upon u_m and the second term on $\mathrm{u}_m, \mathrm{u}_{m-1}$ and so on. Therefore the necessary condition for $\mathbf{Hy}$ to lie inside the sphere of radius d is, $\mathrm{d}'^2 \geq (\mathrm{x}_m - \mathrm{r}_{m,m}\mathrm{u}_m)^2$. Or the condition on u_m can be written as,

$$\left\lceil \frac{-\mathrm{d}' + \mathrm{x}_m}{\mathrm{r}_{m,m}} \right\rceil \leq \mathrm{u}_m \leq \left\lfloor \frac{\mathrm{d}' + \mathrm{x}_m}{\mathrm{r}_{m,m}} \right\rfloor, \tag{4.10}$$

where $\lceil . \rceil$ and $\lfloor . \rfloor$ denotes the rounding off by the nearest largest and smallest integers respectively. Similarly, for every u_m satisfying eq (4.10), there exist a u_{m-1} such that,

$$\left\lceil \frac{-\mathrm{d}'_{m-1} + \mathrm{x}_{m-1|m}}{\mathrm{r}_{m-1,m-1}} \right\rceil \leq \mathrm{u}_{m-1} \leq \left\lfloor \frac{-\mathrm{d}'_{m-1} + \mathrm{x}_{m-1|m}}{\mathrm{r}_{m-1,m-1}} \right\rfloor, \tag{4.11}$$

for, $(\mathrm{d}'_{m-1})^2 = \mathrm{d}'^2 - (\mathrm{x}_m - \mathrm{r}_{m,m}\mathrm{u}_m)^2$ and $\mathrm{x}_{\mathrm{m-1|m}} - \mathrm{r}_{m-1,m}\mathrm{u}_m$. In a similar way one can reach the bottom of the search tree, i.e., u_1. Therefore, instead of searching all the lattice points the search has confined within the sphere of distance d, decreasing the complexity of Maximum likelihood detector.

The sphere decoding algorithm [26] is jotted down in the steps written below.

Algorithm

Input: $\mathrm{Q} = [\mathrm{Q}_1\ \mathrm{Q}_2],\ \mathrm{R},\ \mathbf{y},\ \mathbf{z} = Q_1^*\mathbf{y},\ \mathrm{d}.$

1. Set $k = m$, $(\mathrm{d}'_m)^2 = \mathrm{d}^2 - ||\mathrm{Q}_2{}^*\mathbf{y}||^2, \mathrm{x}_{m|m+1} = \mathrm{x}_m$.
2. (Bounds for u_k) set $\mathrm{UB}(\mathrm{u}_k) = \left\lfloor \frac{\mathrm{d}'_k + \mathrm{x}_{\mathrm{k|k+1}}}{\mathrm{r}_{\mathrm{k,k}}} \right\rfloor$, $\mathrm{u}_k = \left\lceil \frac{\mathrm{d}'_k + \mathrm{x}_{k|k+1}}{\mathrm{r}_{\mathrm{k,k}}} \right\rceil$-1.
3. (Increase u_k), $\mathrm{u}_k = \mathrm{u}_k + 1$. If $\mathrm{u}_k \leq \mathrm{UB}(\mathrm{u}_k)$ go to 5; else, move to 4.

4. (Increase k), $k = k + 1$; if $k = m + 1$ terminate algorithm, else go to 3.

5. (Decrease k) if k=1, go to 6; else $k = k - 1$,
$\mathrm{x}_{k|k+1} = \mathrm{x}_k - \sum_{j=k+1}^{m} \mathrm{r}_{k,j}\mathrm{u}_j, (\mathrm{d}'_k)^2 = (\mathrm{d}'_{k+1})^2 - (\mathrm{x}_{k+1|k+2} - \mathrm{r}_{k+1,k+1}\mathrm{u}_{k+1})^2$,
go to step 2.

6. Solution found. Save $\mathbf{u}$ and its distances from $\mathbf{y}$,
$(\mathrm{d}'_m)^2 - (\mathrm{d}'_1)^2 + (\mathrm{x}_1 - \mathrm{r}_{1,1}\mathrm{u}_1)^2$, go to step 3.

The sphere decoder provides the estimated sequence $\hat{\mathbf{u}}$. We compared the data symbol sequence $\mathbf{u}$ of length N=6 with different cases for the value of L. Where L was chosen as 6, 5 and 4 for three different cases, L = 6 is the Nyquist case for comparison and L =5, 4 are the FTN cases. A sub-optimal MMSE based receiver has also been included for comparing the results. Fig. 4.3 represents the simulation results for the bit error rates vs $\frac{\mathrm{E_b}}{\mathrm{N_0}}$.

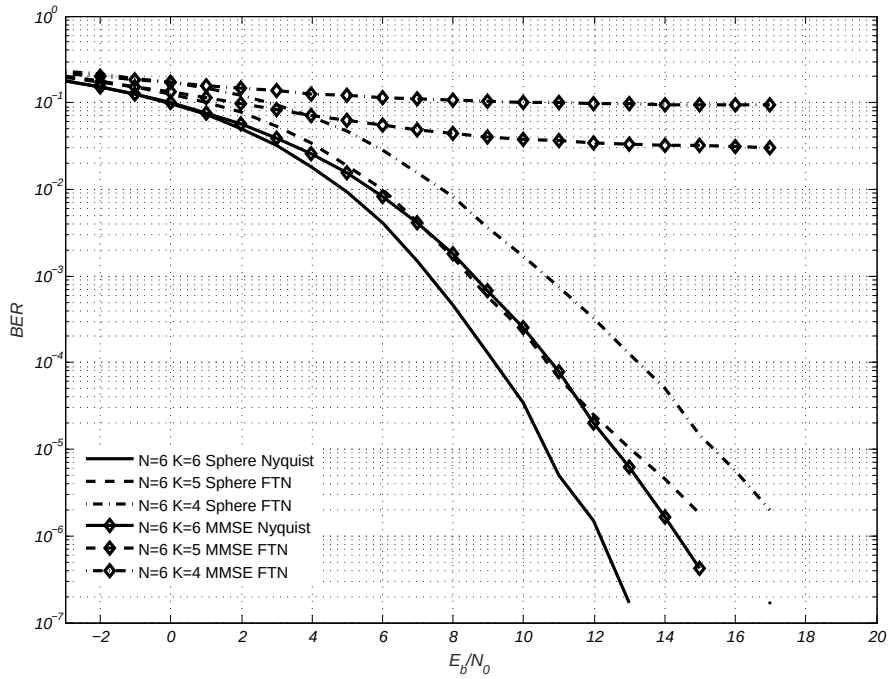

Figure 4.3: BER vs $\frac{\mathrm{E_b}}{\mathrm{N_0}}$ curves for different cases. The diamond carrying curves represent the sub-optimal MMSE based decoding and the rest represents sphere decoding.

The Nyquist based optimal sphere decoding performed the best followed by the Nyquist based sub-optimal MMSE decoding overlapping with the FTN based optimal sphere decoding with L=5, i.e., $\approx 17\%$ faster than the Nyquist rate. Then comes the FTN based optimal sphere decoding with L=4, i.e, $\approx 34\%$ faster than the Nyquist rate. The FTN based MMSE decoding failed to perform. For $\mathrm{P_b} = 10^{-5}$, Nyquist based sphere decoding requires $\frac{\mathrm{E_b}}{\mathrm{N_0}} \approx 10.5$ dB, both Nyquist based MMSE decoding and FTN (with L=5) sphere decoding requires $\frac{\mathrm{E_b}}{\mathrm{N_0}} \approx 12.5$ dB and FTN (with L=4) sphere decoding requires $\frac{\mathrm{E_b}}{\mathrm{N_0}} \approx 15.5$ dB.

4.1.2 Capacity and Spectral efficiency

The *capacity* of discrete time signals with ISI is considered here. Assume input and output relation according to the Forney signal model, given by,

$$\mathbf{y} = \mathrm{H}\mathbf{u} + \mathbf{w}, \tag{4.12}$$

where $\mathbf{y}$ is the received signal vector of size B×1, H is the channel matrix of size B×N, $\mathbf{u}$ is the equiprobable i.i.d input symbol vector of size N×1 and $\mathbf{w}$ is a size B×1 vector containing complex white Gaussian noise samples. The capacity calculation is the mathematical problem to compute mutual information $\mathrm{I}(\mathbf{u};\mathbf{y})$ between input $\mathbf{u}$ and output $\mathbf{y}$.

The constrained capacity [28] (where the constraint is that the mutual information is evaluated for a given discrete PAM/QAM discrete constellation rather than the Gaussian.) for the discrete time ISI Gaussian channel can be given by,

$$\begin{aligned} \mathrm{C_{DT}} &= \frac{1}{\mathrm{N}}\mathrm{I}\left(\mathbf{y};\mathbf{u}\right), \\ &= \frac{1}{\mathrm{N}}\left[\mathrm{H}(\mathbf{y}) - \mathrm{H}(\mathbf{r}|\mathbf{u})\right], \\ &= \frac{1}{\mathrm{N}}[\mathrm{H}(\mathbf{y}) - \mathrm{H}(\mathbf{w})], \end{aligned}$$

where $\mathrm{H}(\cdot)$ is defined as the differential entropy function. Further, $\mathrm{C_{DT}}$ is given by,

$$\mathrm{C_{DT}} = \frac{1}{\mathrm{N}}[\mathrm{H}(\mathbf{y}) - \mathrm{H}(\mathbf{w})] = -\mathbb{E}[\log_2\left(\mathrm{p}(\mathbf{y})\right)] - [\log_2(\pi \mathrm{e N_0})] \times \mathrm{B}. \tag{4.13}$$

Where $\mathrm{C_{DT}}$ has the units bits/sec. The simulation results for the capacity calculation are shown in Fig. 4.4.

The capacity of the Nyquist system with N=L=6 outperforms the capacities of FTN systems with L=5 and L=4 respectively for all the values of $\frac{P}{N_0}$, where $P = E_b R$ for bit rate R. However after $\frac{P}{N_0}$=14 dB all the capacity curves merge to the highest possible value of 12 bits/sec, i.e., the capacity cap. Now, what comes next is spectral efficiency, i.e., the number of transmitted bitots/sec in a unit frequency use.

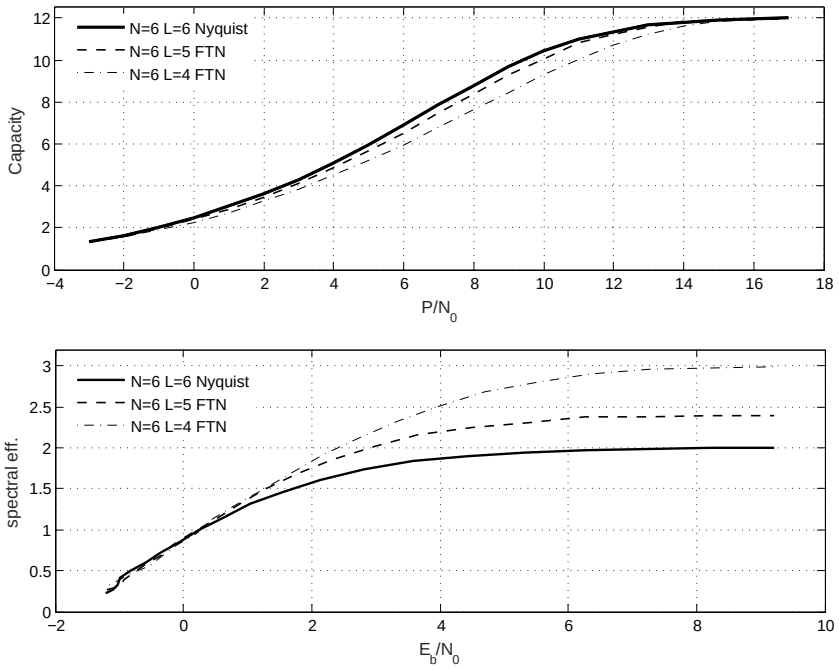

Figure 4.4: Uncoded FTN capacity vs $\frac{P}{N_0}$, spectral efficiency vs $\frac{E_b}{N_0}$

The spectral efficiency of FTN systems outperforms the Nyquist system both for L=5 and L=4. We have derived the spectral efficiency directly from the capacity curve, such that, spectral efficiency=$\frac{\text{capacity}}{\text{bandwidth}}$. The bandwidth for the considered systems is equal to their respective value of L. Similarly, for the fair comparison the x-axis taken is $\frac{E_b}{N_0}$ derived from dividing $\frac{P}{N_0}$ by C. The bottom part of Fig. 4.4 shows this comparison for Nyquist system versus FTN systems. Spectral efficiency is the true parameter for comparing communication systems as it includes the data rate per unit of bandwidth. The FTN system may fall behind in the case of capacity as it was consuming less bandwidth in comparison to the Nyquist system.

4.2 Coded FTN and its detection

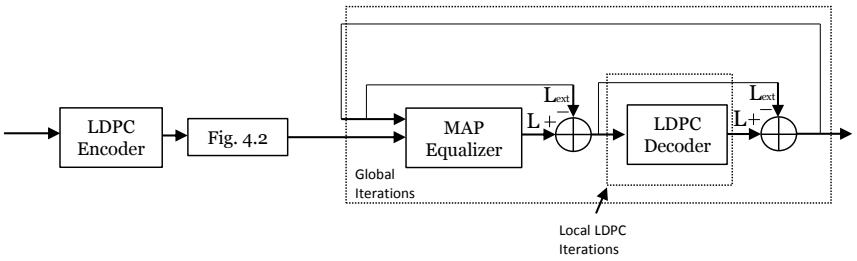

Figure 4.5: LDPC based FTN system model

A coded FTN system is shown in Fig. 4.5. The transmitter consists of an LDPC encoder of code rate $\mathrm{R_c} = 1/2$ producing an encoded bit sequence $\mathbf{x}$ of length $\mathrm{K_v} \log_2 \mathrm{M}$, after passing through the constellation mapper yield a coded symbol sequence $\mathbf{v}$ of length $\mathrm{K_v}$. The block containing Fig. 4.2 represents the entire uncoded transceiver starting from the DFT block till the whitening filter at the receiver side.

Let's define $\mathbf{x}$ as a vector of length $\mathrm{K_v} \log_2 \mathrm{M}$ containing encoded bits, $\mathbf{x}$ is divided into blocks of length $\log_2 \mathrm{M}$ to map the every $\log_2 \mathrm{M}$ encoded bits in to M-ary symbol.

$$\mathbf{x} \triangleq [\mathbf{x}_1, \mathbf{x}_2, \ldots, \mathbf{x}_{\mathrm{K_v}}],$$

$$\mathbf{x}_k \triangleq [\mathrm{x}_{k,1}, \mathrm{x}_{k,2}, \ldots, \mathrm{x}_{k,\log_2 \mathrm{M}}] \text{ for } \mathrm{x}_{k,j} \in [0, 1].$$

The constellation mapper maps $\mathbf{x}_k$ to a symbol v_k from M-ary symbol alphabet $\mathcal{A}$. Let's define coded symbol sequence $\mathbf{v} \triangleq [\mathrm{v}_1, \mathrm{v}_2, \ldots, \mathrm{v}_{\mathrm{K_v}}]$, the sequence $\mathbf{v}$ is divided into small blocks of length N and each block is pass through FTN system explained in the previous section. It is a scenario where multiple coded blocks are being sent through FTN system. Here, $\mathbf{v}$ can be viewed as,

$$\mathbf{v} = [\mathbf{u}_1, \mathbf{u}_2, \ldots, \mathbf{u}_{\frac{\mathrm{K_v}}{\mathrm{N}}}],$$

where,

$$\mathbf{u}_n = [\mathrm{v}_{1+(n-1)\mathrm{N}}; \mathrm{v}_{2+(n-1)\mathrm{N}}; \ldots; \mathrm{v}_{n\mathrm{N}}] \qquad \text{for} \qquad n \in [1, \frac{\mathrm{K_v}}{\mathrm{N}}].$$

The discrete AWGN model can be written as,

$$\mathbf{r}_n = \mathrm{H}_n \mathbf{u}_n + \mathbf{w}_n, \tag{4.14}$$

where $\mathbf{r}_n$ forms a set of sufficient statistics to estimate $\mathbf{u}_n$.

4.2.1 Decoding

Let $\mathrm{L}(\mathrm{x}_{k,j})$ be the a prior information which is being feed to the SISO MMSE equalizer by the LDPC decoder. For the first global iteration $\mathrm{L}(\mathrm{x}_{k,j}) = 0$. A SISO MMSE equalizer computes the a posteriori probabilities $\mathrm{L}(\mathrm{x}_{l,j}|\mathbf{r}_n)$.

$$\mathrm{L}(\mathrm{x}_{k,j}|\mathbf{r}_n) = \log \frac{\mathrm{P}(\mathrm{x}_{k,j}=0|\mathbf{r}_n)}{\mathrm{P}(\mathrm{x}_{k,j}=1|\mathbf{r}_n)} = \log \frac{\sum_{\mathrm{x}:\mathrm{x}_{k,j}=0} \mathrm{p}(\mathbf{r}_n|\mathbf{x})\mathrm{P}(\mathbf{x})}{\sum_{\mathrm{x}:\mathrm{x}_{k,j}=1} \mathrm{p}(\mathbf{r}_n|\mathbf{x})\mathrm{P}(\mathbf{x})}.$$

Now, the SISO MMSE equalizer first computes the estimates of sent symbols $\tilde{\mathbf{u}}_n$ from the MMSE based linear filter and then a posteriori probabilities $\mathrm{L}(\mathrm{x}_{k,j}|\tilde{\mathbf{u}}_n)$ based on the estimated symbols.

$$\mathrm{L}(\mathrm{x}_{k,j}|\tilde{\mathbf{u}}_n) = \log \frac{\mathrm{P}(\mathrm{x}_{k,j}=0|\tilde{\mathbf{u}}_n)}{\mathrm{P}(\mathrm{x}_{k,j}=1|\tilde{\mathbf{u}}_n)} = \log \frac{\sum_{\mathrm{x}:\mathrm{x}_{k,j}=0} \mathrm{p}(\tilde{\mathbf{u}}_n|\mathbf{x})\mathrm{P}(\mathbf{x})}{\sum_{\mathrm{x}:\mathrm{x}_{k,j}=1} \mathrm{p}(\tilde{\mathbf{u}}_n|\mathbf{x})\mathrm{P}(\mathbf{x})},$$

by breaking the above equation into two parts,

$$\mathrm{L}(\mathrm{x}_{k,j}|\tilde{\mathbf{u}}_n) = \log \frac{\sum_{\mathrm{x}:\mathrm{x}_{k,j}=0} \mathrm{p}(\tilde{\mathbf{u}}_n|\mathbf{x}) \prod_{j' \neq j} \mathrm{P}(\mathrm{x}_{k'j'})}{\sum_{\mathrm{x}:\mathrm{x}_{k,j}=1} \mathrm{p}(\tilde{\mathbf{u}}_n|\mathbf{x}) \prod_{j' \neq j} \mathrm{P}(\mathrm{x}_{k'j'})} + \mathrm{L}(\mathrm{x}_{k,j}). \tag{4.15}$$

Therefore a posteriori probabilities $\mathrm{L}(\mathrm{x}_{k,j}|\mathbf{r}_n)$ about the received signal is calculated from the estimated $\mathrm{L}(\mathrm{x}_{k,j}|\tilde{\mathbf{u}}_n)$. $\mathrm{L}(\mathrm{x}_{k,j}|\tilde{\mathbf{u}}_n)$ is calculated by the sum of LLR's, externally fed $\mathrm{L}_{\mathrm{ext}}$ and L_{e} which is the right part of eq. (4.9) and is independent of $\mathrm{L}_{\mathrm{ext}}$. Calculated $\mathrm{L}(\mathrm{x}_{k,j}|\tilde{\mathbf{u}}_n)$ is then fed to the LDPC decoder with subtracted $\mathrm{L}_{\mathrm{ext}}$. LDPC decoder produces a posteriori LLR $\mathrm{L}(\mathrm{x}_{l,j})$ which are feed back to the MMSE equalizer improving the decision on $\mathbf{r}_n$. Finally after a pre decided number of iterations we get the estimated bit sequence $\hat{\mathbf{x}}$.

We have compared the Nyquist system for block length N=6 with the two cases of FTN systems having L=5 and L=4, i.e., deleting one and two frequency symbols respectively. The modulation considered is QPSK. Fig. 4.6 shows the BER vs $\frac{\mathrm{E_b}}{\mathrm{N_0}}$ comparison between the Nyquist and FTN cases.

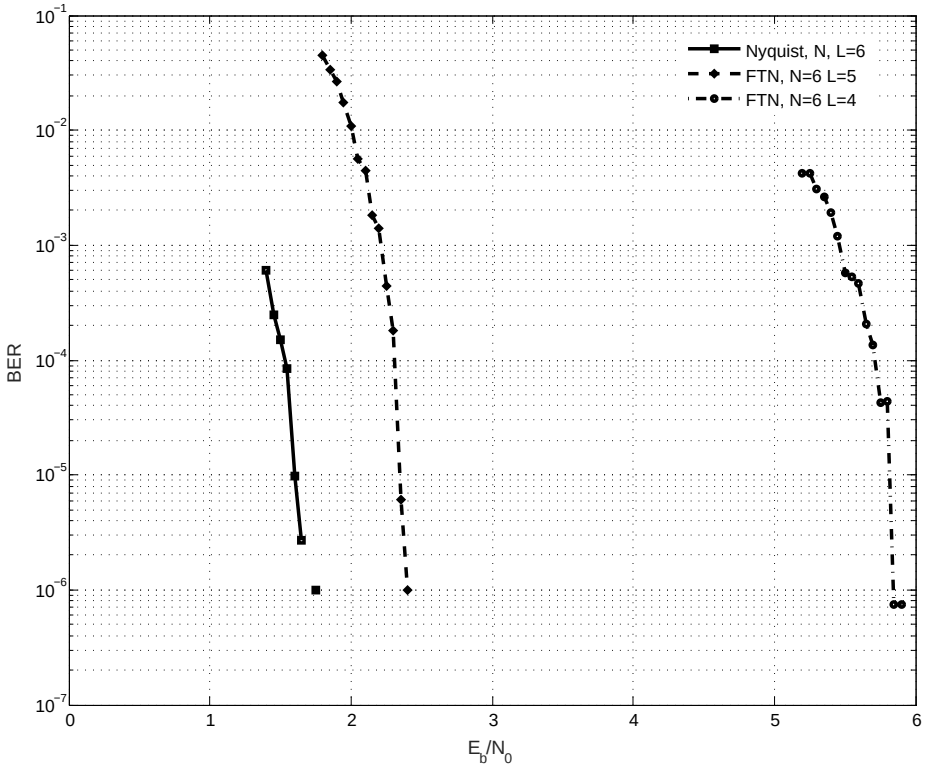

Figure 4.6: BER vs $\frac{E_b}{N_0}$ performance comparison between the coded Nyquist and coded FTN cases. The modulation scheme is QPSK.

The Nyquist case performed best with the left most curve, FTN with L=5 is the curve shown in the middle and far right is the FTN system with L=4. FTN with L=5 witnessed an increase in the data rates up to $(6-5)/6 \times R_c \times \log_2 M \approx 17\%$ and $(6-4)/6 \times R_c \times \log_2 M \approx 33\%$ increase in rate for L=4 case, while keeping the bandwidth W constant. For a BER of 10^{-5}, the Nyquist system requires an $\frac{E_b}{N_0} \approx 1.6$ dB, whereas the FTN system with L=5 requires an $\frac{E_b}{N_0} \approx 2.4$ dB. The FTN system with L=4 needs an $\frac{E_b}{N_0} \approx 5.8$ dB. FTN system with L=5 requires 0.8 dB more $\frac{E_b}{N_0}$ in comparison to the Nyquist system while there is a need of 4.2 dB more $\frac{E_b}{N_0}$ for L=4 case. This result was quite expected as with the FTN an additional ISI occurs resulting in more errors at the receiver side. Fig. 4.7 shows the comparison of spectral efficiency of the Nyquist system and FTN systems.

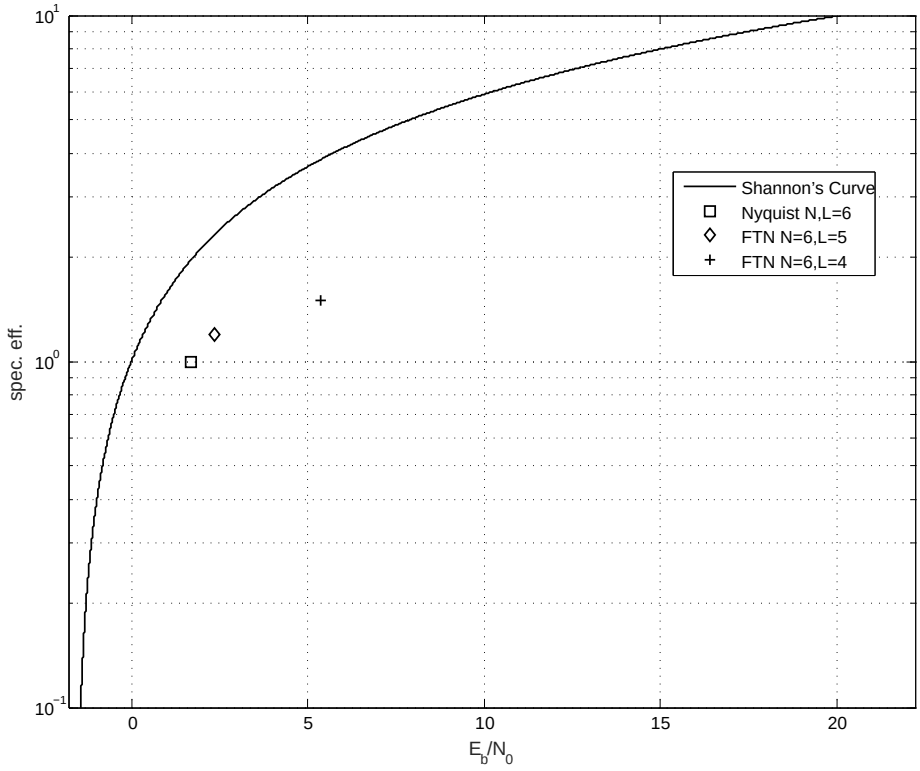

Figure 4.7: Spec. eff. vs $\frac{E_b}{N_0}$ for a BER of order 10^{-5}.

With an LDPC encoder with code rate $R_c = \frac{1}{2}$, the spectral efficiency of the Nyquist system with QPSK modulation is 1, similarly FTN cases with L=5 and L=4 with QPSK modulation can carry 1.2 bits/sec/Hz and 1.5 bits/sec/Hz respectively. The FTN systems performed better than the Nyquist system but they require more $\frac{E_b}{N_0}$ as can be seen in Fig. 4.7. Therefore to gain additional spectral efficiency one has to pay in the form of $\frac{E_b}{N_0}$ even in the case of FTN.

Chapter 5

Conclusion and Future Work

The faster than Nyquist signaling is an alternate way of increasing data rate without the expense of bandwidth or transition to higher modulation order. We have successfully modelled the faster than Nyquist signaling on LTE-uplink like system models. In this thesis we chose an alternate way of implementing FTN by deleting some frequency symbols and try to recover them at the receiver side. The results we got were not very promising, we were expecting better results for the BER performances. One thing to be noted is that the value of N and L we chose were very small, for example when L =5 for N = 6 there is a direct $\approx$ 17% increase in data rate which is quite a big value. By choosing larger and more practical values of N and comparing the system with different L's, so that there won't be an abrupt increase in data rate. This can be a point to look after in the future studies. Also, the conventional way of implementing FTN by increasing the rate of pulse shaping filter is another possibility in future studies.

In the coded case our receiver was not completely optimal, since we used a sub-optimal MMSE based SISO equalizer. Using a optimal equalizer cascaded with an LDPC decoder can further improve our results. Since this work is a preliminary study, this option could be exploited in the future. The FTN signaling is already extended in the frequency domain in [23]. Therefore, multi-dimensional FTN in the LTE-uplink like system models is also a possible case of study.

References

[1] C. E. Shannon, "A mathematical theory of communication", *Bell Syst. Tech. J.*, vol.27, pp. 379-423, July 1948, and pp. 623-657, Oct. 1948.

[2] H. Nyquist, "Certain factors affecting telegraph speed", *Bell Syst. Tech. J.*, pp. 324-346, April 1924.

[3] J. E. Mazo, "Faster than Nyquist signaling", *Bell Syst. Tech. J.*, pp.1451-1462, Oct. 1975.

[4] D. J. Costello, G.D. Forney, Jr., "Channel coding: The road to channel capacity", *Proceeding of IEEE.*, vol.95(6), pp. 1150-1177, June 2007.

[5] N. Wiberg, "Codes and decoding of general graph", *Ph.D. dissertation*, Linkőping Univ., Linkőping, Sweden, 1996.

[6] N. Wiberg, H.A. Loeliger, and R. Kőtter, "Codes and iterative decoding on general graphs", *Eur. Trans. Telecomm.*, vol. 6, pp. 513-525, Sep./Oct. 1995.

[7] H. Kobayashi, "Correlative level coding and maximum-likelihood decoding", *IEEE Trans. Inform. Theory*, vol.17(5), pp. 586-594, Sep. 1971.

[8] G. D. Forney, Jr., "Maximum-likelihood sequence estimation of digital sequences in the presence of intersymbol interference", *IEEE Trans. Inform. Theory*, vol.18(2), pp. 363-378, May 1972.

[9] R. Gallager, L. Zheng, "Principles of Digital Communications I, Fall 2006", *Massachusetts Institute of Technology: MIT OpenCourseWare*, License: Creative Commons BY-NC-SA. `http://ocw.mit.edu` (Accessed Dec. 15, 2015).

[10] G. Lindell, "Introduction to Digital Communications", *Lund Univ.*, Compendium Aug. 2006. `http://www.eit.lth.se/course/ett051`, `http://www.eit.lth.se/course/ettn01`.

[11] G. Ungerboeck, "Adaptive maximum-likelihood receiver for carrier-modulated data-transmission systems", *IEEE Trans. Commun.*, vol. 22(5), pp. 624-636, May 1974.

[12] M. Tuchler, A.C. Singer, and R.Koetter, "Minimum mean squared error equalization using a priori information", *IEEE Trans. Signal Processing*, vol. 50(3), pp. 673-683, March 2002.

[13] J.E. Mazo and H.J. Landau, "On the minimum distance problem for faster than Nyquist Signaling", *IEEE Trans. Inform. Theory*, vol. IT-34, pp. 1420-1427, Nov.1988.

[14] D. Hajela, "On Computing the minimum distance for faster than Nyquist signaling", *IEEE Trans. Inform. Theory*, vol. IT-36, pp. 289-295, Mar. 1990.

[15] B. R. Saltzberg, "Intersymbol interference error bounds with application to ideal bandlimited signaling", *IEEE Trans. Inform. Theory*, vol. IT-14, pp. 563-568, July 1968.

[16] A. Fihel and H. Sari, "Performance of reduced-bandwidth 16 QAM with decision-feedback equalization", *IEEE Trans.Commun.*, vol. COM-35, pp. 715-723, July 1987.

[17] G. J. Foschini, "Contrasting performance of faster binary signaling with QAM", *Bell Syst. Tech. J.*, vol. 63, pp. 1419-1445, Oct. 1984.

[18] A. Liveris and C. Georghiades, "Exploiting faster than Nyquist signaling", *IEEE Trans. Commun.*, vol. 51, no. 9, pp. 1502âĂŞ1511, Sep. 2003.

[19] Rusek and J. Anderson, "On information rates for faster than Nyquist signaling", *IEEE Global Telecommunications Conference*, GLOBECOM'06, pp. 1-5, Nov. 2006.

[20] –, "Non binary and precoded faster than Nyquist signaling", *IEEE Trans. Commun.*, vol. 56, no. 5, pp. 808-817, May 2008.

[21] J. Anderson and A. Prlja, "Turbo equalization and an M-BCJR algorithm for strongly narrowband intersymbol interference", *Information Theory and its Applications (ISITA), 2010 International Symposium on. IEEE*, pp. 261-266, Oct. 2010.

[22] F. Rusek and J. Anderson, "Constrained capacities for faster than Nyquist signaling", *IEEE Trans. Inform. Theory*, vol. 55, no. 2, pp. 764-775, Feb. 2009.

[23] J. Anderson and F. Rusek, "Improving OFDM: Multistream faster than Nyquist signaling", *6th International ITG-Conference on Source and Channel Coding (TURBOCODING), 2006 4th International Symposium on Turbo Codes & Related Topics.*

[24] C. Berrou, A. Glavieux, and P. Thitimajshima, "Near Shannon limit error-correcting coding and decoding: Turbo-codes. 1", *Proceedings of 1993 International Conference on Communications*, pp. 1064âĂŞ1070, May 1993.

[25] E. Dahlman, S. Parkvall and J. Skold, *4G: LTE/LTE-Advanced for Mobile Broadband-Handbook*, 2nd ed., Elsevier, 2014.

[26] A.P. Clark and U.S. Tint, "Linear and non-linear transversal equalizers for baseband channels", *Radio and Electronic Engineer*, vol. 45, no. 6, pp. 271-283, June 1975.

[27] B. Hassibi, H. Vikalo, "On the sphere-decoding algorithm. I. Expected complexity", *IEEE Trans. Signal Processing*, vol. 53, no. 8, pp. 2806-2818, Aug. 2005.

[28] F. Rusek, "Partial response and faster than Nyquist signaling", *Ph.D. dissertation*, Lund Univ., Lund, Sweden, Sep. 2007.

[29] "Spectral efficiency", *Wikipedia*, 27 Jan. 2015.